T.R.

SAKARYA UNIVERSITY

INSTITUTE OF NATURAL SCIENCES

DESIGN AND ANALYSIS OF A HEAT EXCHANGER FOR A SMALL-SCALE GAS TURBINE

MASTERS DEGREE THESIS

Princely Kolle EPIE

Department	**:**	**AUTOMOTIVE ENGINEERING**
Supervisor	**:**	**Prof. Dr Can HAŞİMOĞLU**

February 2020

T.C.

SAKARYA UNIVERSITY

INSTITUTE OF NATURAL SCIENCE

DESIGN AND ANALYSIS OF A HEAT EXCHANGER FOR A SMALL-SCALE GAS TURBINE

MASTERS DEGREE THESIS

Princely Kolle EPIE

Department : AUTOMOTIVE ENGINEERING

This thesis has been accepted unanimously by the examination committee on 10.02.2020

Prof. Dr.	Prof. Dr.	Prof. Dr.
Murat HOŞÖZ	Can HAŞİMOĞLU	Hakan Serhad SOYHAN
Jury President	Member	Member

DECLARATION

I declare that all the data in this thesis was obtained by myself in academic rules, all visual and written information and results were presented in accordance with academic and ethical rules, there is no distortion in the presented data, in case of utilizing other people's works they were refereed properly to scientific norms, the data presented in this thesis has not been used in any other thesis in this university or in any other university.

Princely Kolle EPIE

…..__.2020

ACKNOWLEDGEMENT

This thesis work was carried out in the department of Automotive Engineering at Sakarya University, Turkey.

The author would like to express his gratitude to all those who confirmed the permission and thus, made it possible to complete the thesis work, most particularly The Republic of Turkey and The Turks Abroad and Related Communities Presidency.

Most notably, I would like to convey my thanks to my supervisor Prof. Dr. Can HAŞİMOĞLU for his continuous follow-up, support and advice throughout this thesis work. I would also like to thank Assoc. Dr. Gökhan COŞKUN, Prof. Dr. H. Serhad SOYHAN for their support throughout this thesis project.

Last but not the least, I would like to thank my entire family for their unending help and support.

TABLE OF CONTENTS

LIST OF SYMBOLS AND ABBREVIATIONS

PHE	: Plate Heat Exchanger
PFHE	: Plate Fin Compact Heat Exchanger/ Plain-Fin Compact Heat Exchanger
PCHE	: Printed Circuit Heat Exchanger
SHE	: Spiral Heat Exchanger
CHE	: Compact Heat Exchanger
AMT	: Arithmetic Mean Temperature, K
NTU	: Number of Transfer Unit
R	: Gas constant, kJ/kmol. K,
Re	: Reynolds number
ΔP	: Pressure drop, Pa
Q	: Heat transfer, J
G	: Core velocity, kg/m^2
A	: Total surface area, m^2
A_o	: Free flow area, m^2
A_{fr}	: Frontal area, m^2
T	: Temperature, K
i/o	: Inlet/Outlet
c	: Cold air
h	: Hot gas
k	: Ratio of specific heats
C_p/C_t	: Specific heat at constant pressure/temperature, J/kg
j/f factor	: Friction correlation factors
P	: Pressure, Pa
ε	: Effectiveness

$b_h = b_c$	: Fin height, m
δ_w	: Fin thickness, m
$\beta_c = \beta_h$	: Heat transfer surface area density, m^2/m^3
$\left(\frac{A_f}{A}\right)_h = \left(\frac{A_f}{A}\right)_c$	: Fin area/total area ratio, dimensionless
$D_{h,h} = D_{h,c}$	: Hydraulic diameter, m
$\dot{m}_h$	: Fluid mass flow rates, kg/s
ΔP_h	: Pressure drop, Pa
k_w	: Plate Thermal heat transfer, W/m
$T_{h,i}$	: Inlet Temperatures of gases, K
$T_{h,O}$	: Outlet Temperatures of gases, K
$T_{c,i}$	: Inlet Temperatures of air, K
$T_{c,O}$	: Outlet Temperatures of air, K
η_o	: Overall Surface Efficiency
U	: Overall Heat Transfer Coefficient, $W/m^2.K$
A	: Total Surface Area, m^2
Q	: Heat Transfer between Fluids, W

LIST OF FIGURES

LIST OF TABLES

SUMMARY

Keywords: Heat recuperator, gas turbine, design, plain fin compact heat exchanger

A gas turbine is classified as a continuous combustion internal combustion engine. Small scale gas turbines are gas turbines with an output of up to 500 kW. These internal combustion engines unlike the traditional Otto and Diesel engines, work following the Brayton cycle. For these engines to achieve high efficiencies values of about 50%, with an electrical efficiency of about 35%, they need to be run with a recuperated energy cycle of varying configurations. Thus, the objective of this work is to design a heat exchanger for a small-scale gas turbine.

In this work, we are aiming at increasing the efficiency of an already existing small-scale gas turbine. This will be done by incorporating it with a Plain-Fin Compact Heat Exchanger (PFCHE). This PFCHE is of rectangular fins and a crossflow fin arrangement. The material of construction is steel due its high thermal resistance. The design of the heat exchanger was done based on the algorithm given by Shah et al. This design was then implemented using an appropriate CAD tool. From the design, simulation tests were run using a full adaptive and automatic meshing algorithm. This simulation results were then analysed. It was found that there was a 32% rise in the temperature of the air entering the combustion chamber of the turbine. Also, a 50% reduction in the fin height can cause as much as an 18% increase in the fin efficiency of the heat exchanger, while a 50% increase in the effectiveness value can cause as much as a 40% increase in the outlet temperature.

KÜÇÜK ÖLÇEKLİ BİR GAZ TÜRBİNİ İÇİN ISI DEĞİŞTİRİCİ TASARIMI VE ANALİZİ

ÖZET

Anahtar Kelimeler: Isı geri kazanıcı, gaz türbini, tasarım, düzlen kanatlı kompakt ısı değiştirici

Bir gaz türbini, sürekli yanmalı içten yanmalı bir motor türüdür. Küçük ölçekli gaz türbinleri, 500 kW'a kadar güç üreten gaz türbinleridir. Bu içten yanmalı motorlar, geleneksel Otto ve Diesel motorlarının aksine, Brayton çevrimine göre çalışır. Bu gaz türbinlerinin, yaklaşık %50'lik yüksek verimlilik değerlerine ve yaklaşık %35'lik elektrik verimliliğine ulaşmak için geri kazanılmış bir enerji döngüsü ile çalıştırılması gerekir. Bu çalışmanın amacı, küçük ölçekli bir gaz türbininin verimliliğini artıracak bir ısı eşanjörü tasarlamaktır.

Bu çalışmada, halihazırda mevcut olan küçük ölçekli bir gaz türbininin verimliliğinin arttırılması hedeflenmiştir. Bu, bir düzlem kanatlı Kompakt Isı Eşanjörü (PFCHE) ile birleştirilerek yapılmaktadır. Bu PFCHE, dikdörtgen kanatlardan ve bir çapraz akış kanat düzeninden oluşmaktadır. Ana malzeme, yüksek ısı direnci nedeniyle çeliktir. Isı eşanjörünün tasarımı Shah ve diğ. tarafından verilen algoritmaya göre yapılmıştır. Bu tasarım daha sonra uygun bir CAD aracı kullanılarak gerçekleştirilmiştir. Geliştirilen tasarımın, simülasyon testleri tam uyarlamalı ve otomatik bir mesh algoritması kullanılarak yapılmıştır. Bu simülasyon sonuçları daha sonra analiz edildmiş ve türbinin yanma odasına giren havanın sıcaklığında %32'lik bir artış olduğu bulunmuştur. Ayrıca, kanatçık yüksekliğinde %50'lik bir azalmanın, ısı eşanjörünün kanatçık veriminde %18'e kadar bir artışa neden olabileceği belirlenmiştir. Ayrıca, etkinlik değerinde %50'lik bir artışın, çıkış sıcaklığında %40 kadar bir artışa neden olabileceği tespit edilmiştşr.

CHAPTER 1 . INTRODUCTION

1.1. Compact Heat Exchangers

A heat exchanger having a surface area thickness more prominent than around 700 m^2/m^3 is subjectively alluded to as a compact heat exchange [1]. Compact heat exchangers are mostly used in industrial processes and engines where gas-to-gas or liquid-to-gas heat exchange is required. Some of these processes are; vehicular heat exchangers, condensers and evaporators in air-conditioning and refrigeration industry, aircraft oil coolers, automotive radiators, oil coolers, unit air heaters, intercoolers of compressors, offshore and onshore power plants, cryogenics, and aircraft and space applications.

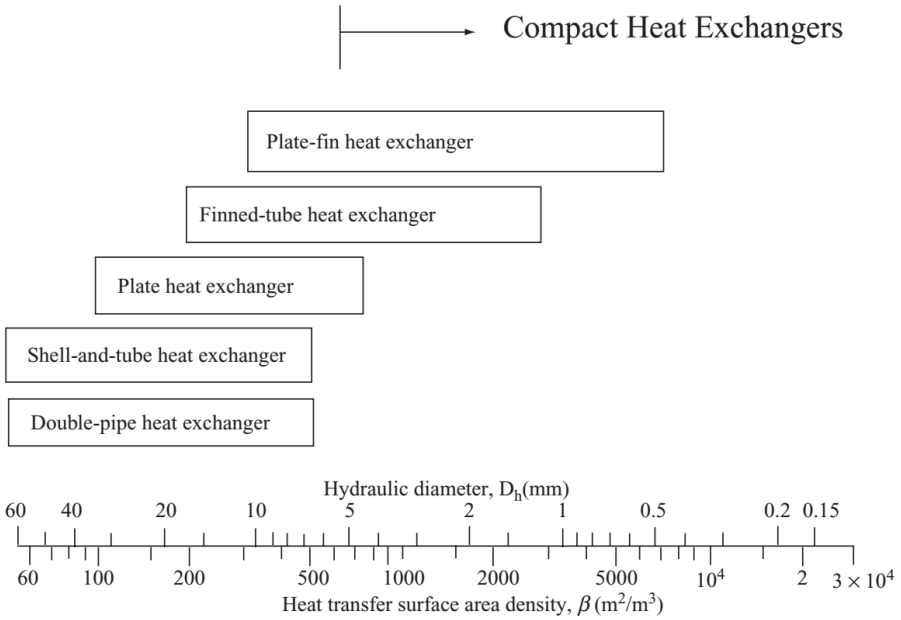

Figure 1.1. Overview of The Compactness of Heat Exchangers [2].

1.2. Characteristics of Compact Heat Exchangers

Some specific characteristics of heat compact exchangers are as follows [2].

1. Usually with expanded surfaces.
2. A high heat transfer surface area per unit volume of the core, for the most part of more than 700 m^2/m^3 on at least one of the fluid sides which usually has gas flow.
3. Small hydraulic diameter.
4. Usually most likely one of the fluids is a gas.
5. Fluids must be clean and relatively non-fouling because of small hydraulic diameters (D_h) flow passages and difficulty in cleaning.
6. The fluid pumping power (i.e., pressure drop) consideration is as important as the heat transfer rate.
7. Operating weights and temperatures are restricted to a limited degree when contrasted with shell and tube exchangers because of slender fins as well as joining of the fins to plates or tubes by brazing, mechanical development, and so on.
8. Fluid contamination is commonly not an issue.
9. Flexibility in disseminating surface region on the hot or cold side as wanted by the designer.
10. Variety of surfaces are accessible having various orders of magnitudes of surface area density.

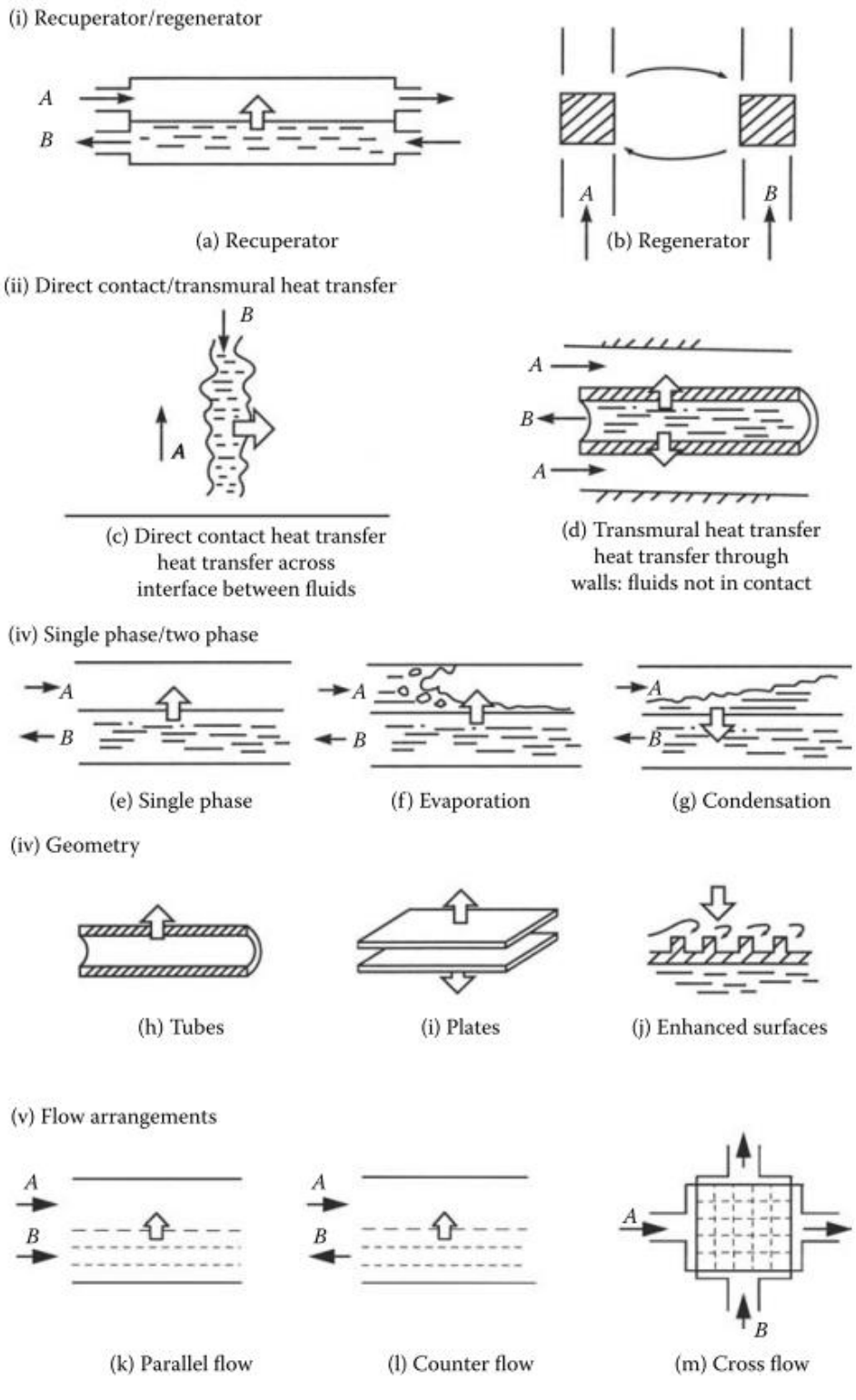

Figure 1.2. Criteria Used In The Classification Of Heat Exchangers.[1].

1.3. Types of Compact Heat Exchangers

Compact heat exchangers have witnessed a large variety of plate fin geometries. Nonetheless, more of these geometries are still being developed. Some of these geometries are presented below

1.3.1. Plate and frame heat exchangers (PHE)

These heat exchangers are made of a progression of layered plates. These plates are typically bolstered by unbending frames which structure exceptionally interrupted channels [3]. PHEs have the accompanying points of interest; minimization, high heat transfer efficiencies, high heat transfer coefficients, high effectiveness, can work at high temperatures and pressure and effectively cleaned. The primary disadvantages of the PHEs are their limitation to direct temperature and pressure applications because of their utilization of gaskets. Additionally, for proportionate flow velocities, the pressure drop in a PHE is generally high because of its limited entries which can be obstructed by particulate contaminants in the liquid, and incapable transverse vortices and crisscross flow designs [4]. Figure 1.3. shows an exploded view of a Plate and Frame Heat Exchanger. Table presents the different types of PHE and their characteristics [3].

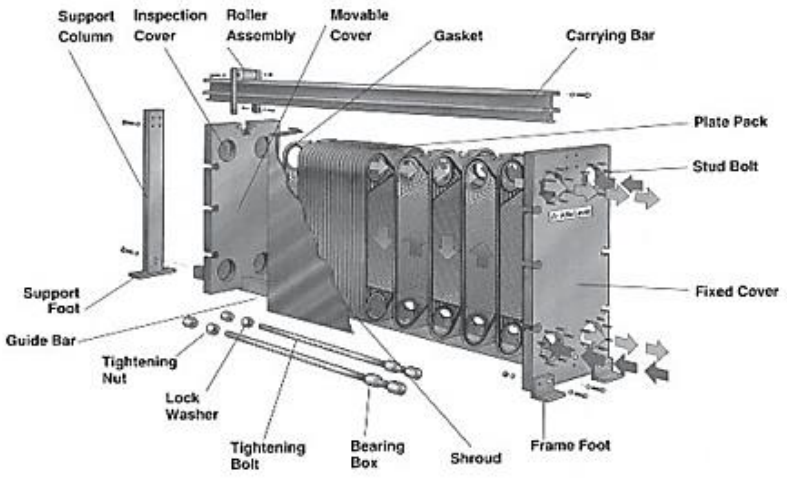

Figure 1.3. An exploded view of a PHE (courtesy of Alfa Laval).[5].

Table 1.1. Types of Compact Heat Exchangers and their characteristics.[3]

Type of PHE	**Characteristics**
Gasketed	Utilized all through the process industry as standard gear for efficient heating, cooling, heat recuperation, condensation, and dissipation.
Wide-Gap Gasketed	Utilized for general heating, cooling and heat recuperation of media containing strands and coarse particles. This sort is additionally reasonable for exceptionally viscous liquids.
Double-Wall Gasketed	It keeps liquids from intermixing and joins the high-efficiency heat transfer advantages of traditional plates with a design that takes out the danger of mixing.
Semi-Welded Gasketed	Are for use in applications where it is hard to locate a good gasket, for example, acid and ammonia; and where there is less hazard for spillage. This sort handles most refrigerants on the welded side and is especially appropriate for smelling salts activities.
Fully Welded	They are most suitable for high temperature and high-pressure applications.
Welded Circular Plate and Shell	In light of the plate-and-shell idea makes the welded plate-and-shell heat exchanger reasonable for utilizations including high pressures and temperatures.
Compact Welded Plate Bloc	An all-welded plate pack gets rid of all gaskets among plates and makes it conceivable to work with a wide scope of harsh media and at high temperatures and pressures.
Fusion Bonded	This is a 100 % stainless steel, non-gasket elective for modern industrial applications that utilise harsh fluids just as those in which there is a requirement for high productivity, hermetically sealed PHEs.
Spiral	Compactness and an auto-cleaning configuration make spiral heat exchangers flexible. They are appropriate for everything from messy liquids to high vacuum condensation.

1.3.2. Plate-fin heat exchanger (PFHE).

These heat exchangers have high surface densities and can deal with numerous liquid streams (Figure 1.4.). They are for the most part comprised of aluminium, erosion, and heat resistant amalgams, and stainless steel. Their activity points of confinement rely upon the material from which they are made of. This can shift from 473K for cryogenic tasks straight up to 800K for tempered steel activities. The pressure limits as far as

possible can go up to 100 bars for aluminium. PFHE are comprised of blades limited by sidebars that are isolated by flat separating sheets. Because of the need to expand blade efficiency, various kinds of fins have been made; plain fins, wavy and layered fins, offset strip fins, louvered fins, and vortex generator [6] (Table 1.2.) [3].

Figure 1.4. Plate fin heat exchanger [7].

Table 1.2. Types of PFHE and their characteristics. [3]

PFHE Type	Characteristics
Plain Fins	Most usually applied have flow channels with either a rectangular or triangular cross-section. Expanding surface area, plain blades require a thinner flow frontal zone than interfered with surfaces (for example offset strip fins and louvered fins) for given estimations of heat duty, pressure drop, and flow rate, yet they are portrayed by quite ng continuous flow stream passages bringing about a higher overall heat exchanger volume.
Wavy and Corrugated Channel	Because of the configuration of the fins, the flow stream direction would be changed and the boundary layer would be isolated, which causes high thermal execution rate.
Offset Strip Fins	Strip fins (offset fins): the short segments of fins are adjusted completely with the flow direction. Because of the short flow length fins, the boundary layer never turns out to be thick. In this manner, there is a high heat transfer coefficient.
Louvered Fins	Louvered fins: fins are removed and twisted into the stream at regular distances, to break the boundary layers and accomplish high thermal execution rate.
Vortex Generators	Vortex generators do not altogether change the effective heat transfer surface region of the plate, yet they increment the heat transfer coefficient by making longitudinally spiralling vortices which advance blending between the surface and centre regions of the stream. Vortex generators are a moderately new kind of upgrade gadget, and an ideal geometry has not yet been landed at. There are quite a number of potential outcomes for various vortex generator surfaces since one can shift the size, attack angle, perspective proportion, as well as course of action of the vortex generators.

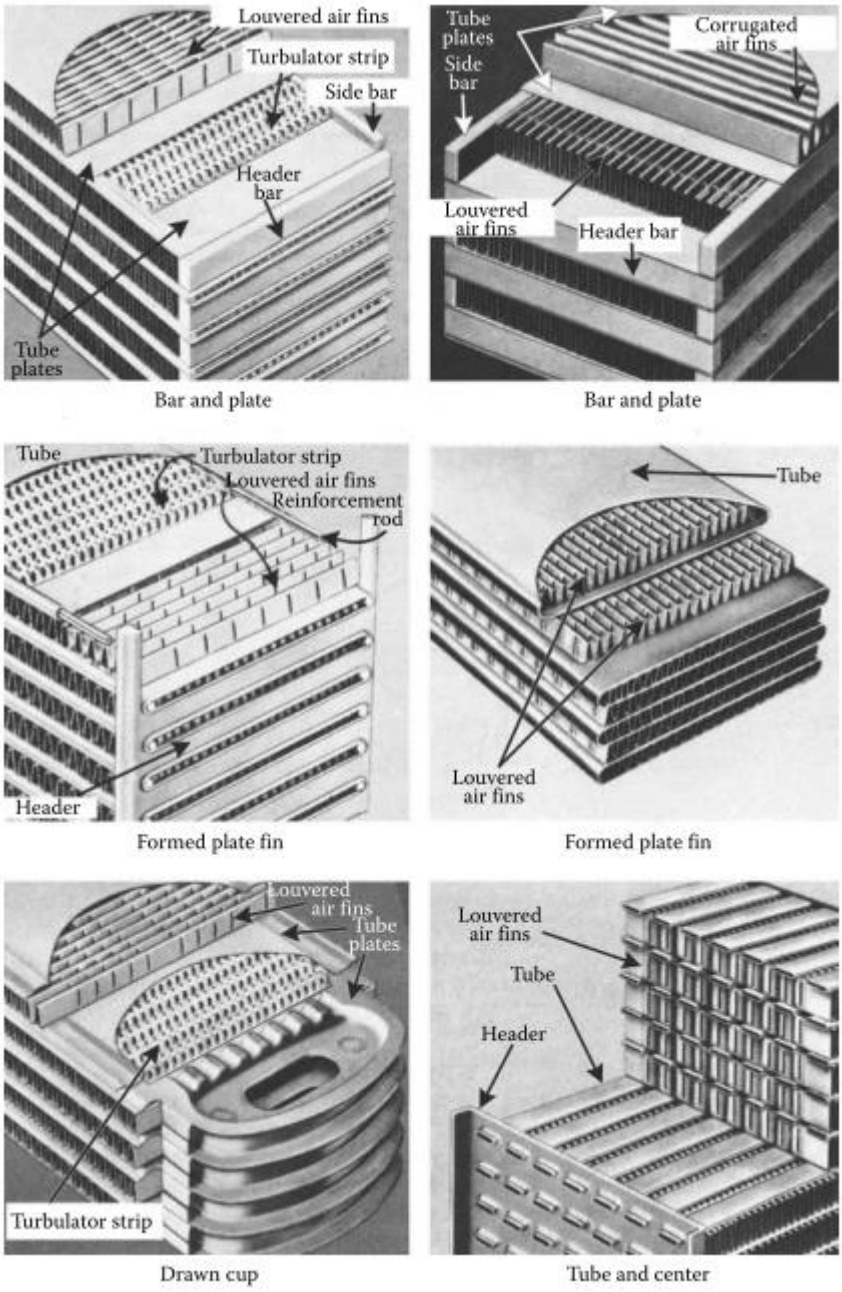

Figure 1.5. Types of PFHEs.[1,2]

1.3.3. Printed circuit heat exchanger (PCHE).

These heat exchangers have a high level of adaptability in their modelling with a high strength because of their method of development. They are normally made out of stainless steel 316L, nickel and titanium [8]. The idea of PCHE empowers concurrent

high temperature and high-pressure activity with moderately slim wall thicknesses between primary and secondary fluid cooling. They can work at pressures up to 500-1000 bar, generally 600 bar and can adapt to extraordinary temperatures extending to 900 ˚C for cryogenics [3].

1.3.4. The Marbond heat exchanger.

In view of a methodology known as Process Intensification (PI), Marbond heat exchanger is the most recent really inventive PCHEs. The assembling techniques of Marbond heat exchanger are like those of the PCHE [3]. The Marbond heat exchangers are considered as high-integrity, high compact blocks ready to work over a scope of pressures and temperatures not met in increasingly ordinary gasketed or welded CHEs. The Marbond unit is fit for being utilized at temperatures inside the range −200 ◦C to 900 ◦C. Pressure differentials more than 400 bars can be contained [3,8].

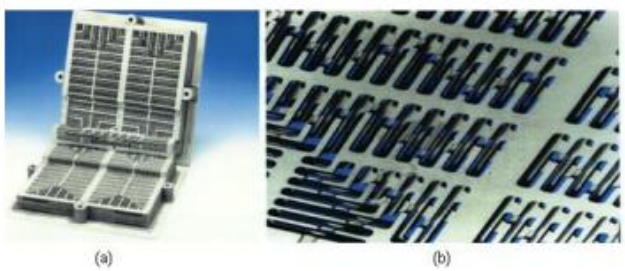

Figure 1.6. Marbond heat exchanger, (a) Exploded view, (b) layers of slotted plates forming flow paths [3].

1.3.5. Spiral heat exchanger (SHE).

These heat exchangers are typically comprised of two long strips of plate wrapped to shape concentric spirals. They are typically made of carbon steel, tempered steel, and titanium. They work at temperatures up to 400 ◦C and pressures of 25 bar contingent upon the gasketing being applied.

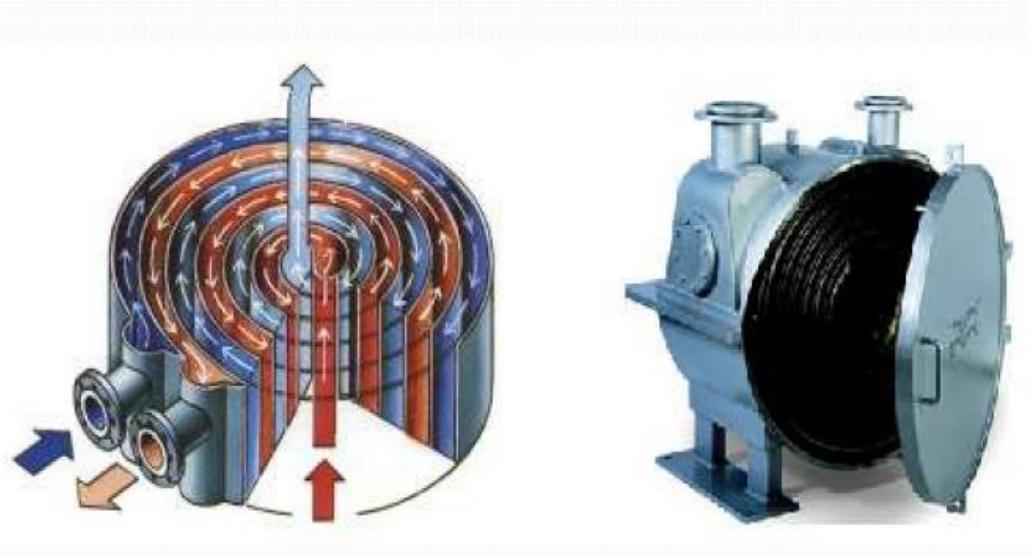

Figure 1.7. Spiral heat exchanger [8].

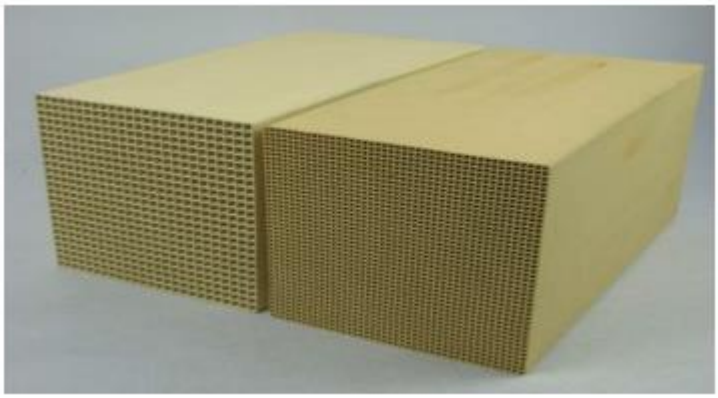

Figure 1.8. Ceramic heat exchanger [8].

1.3.6. Ceramic heat exchanger.

Business CHEs are for the most part fin-and-cylinder or plate-type structures applying copper or aluminium. Notwithstanding, the advances in ceramics, particularly in ongoing 20 years, help the improvement of novel ceramic CHE structures in high-temperature applications [9].

The principle preferences for ceramic materials over conventional metallic materials in CHE development are their amazingly high-temperature resistance, low material expense, and very good corrosion resistance.

Table 1.3. Different Types of Heat Exchangers and their Principal Features. [3]

Types	Features							
	Compactness (m^2/m^3)	Stream types[1]	Materiel[2]	Temperature range (°C)	Max-pressure (bar)	Cleaning methods	Corrosion resistance	Multistram /multipass capacity
Platular plate	200	Gas-liquid, two-phase	s/s, hostelloy, Ni alloys	up to 700	40	Mechanical[4,13]	Good	Yes[14]/Yes
Compabloc Plate	<=300	Liquids	s/s,Ti, Incoloy	up to 300	32	Mechanical[4]	Good	Not.usually/ Yes
Packinox plate	<=300	Gases, liquids, two – phase	s/s, Ti, Hastelloy, Inconel	-200 up to +700	300	Mechanical[4.15]	Good	Yes[6]/Yes
Spiral	<=200	Liquid-liquid, two-phase	c/s, s/s, Ti, Incoloy, Hastelloy	up to 400	25	Mechanical[4]	Good	No/No
Brazed plate-fin	800 up to 1500	Gases, liquids, two – phase	Al, s/s, Ni alloy	Cryogenic to +650	90	Chemical	Good	Yes/Yes
Diffusion-bonded plate-fin	700 up to 800	Gases, liquids, two – phase	Ti, s/s	up to 500	>200	Chemical	Excellent	Yes/Yes

Types	Features							
	Compactness (m^2/m^3)	Stream types[1]	Materiel[2]	Temperature range (°C)	Max-pressure (bar)	Cleaning methods	Corrosion resistance	Multistram /multipass capacity
Plate-and-frame (gaskets)	<=200	Liquid-liquid, gas-liquid, two-phase	s/s, Ti, Incoloy, Hastelloy, graphite, polymer	-35 to +200	25	Mechanical[4]	Good[5]	Yes[6]/Yes
Partially Welded Plate	<=200	Liquid-liquid, gas-liquid, two-phase	s/s, Ti, Incoloy, Hastelloy	-35 to +200	25	Mechanical[4,7] Chimical[8]	Good[5]	No/Yes
Fully welded plate (Alfa Rex)	<=200	Liquid-liquid, gas-liquid, two-phase	s/s,Ti, Ni alloys	-50 to 350	40	Chemical	Good	No/Yes
Brazed plate	<=200	Liquid-liquid, two-phase	s/s	-195 to +220	30	Chimical[9]	Good	No/No[11]
Bavex plate	200 up to 300	Gases, liquids, two – phase	s/s, Ni, Cu, Ti, special steels	-200 to +900	60	Mechanical[4,9] Chemical	Good[10]	In.principe/ Yes

The significant impediments in the improvement of ceramic CHEs basically epitomize in their inherent fragility in pressure, challenges in moulding and fixing and hence high assembling expenses. They cannot withstand enormous heat variations and are vulnerable to thermal shock failures aside from silicon carbide and silicon nitride. Along these lines, most of the studies concentrate on less fragile ceramic variations, for example, composite ceramics. Ceramic matrix composites (CMCs) were created by consolidating reinforced ceramics stages into a ceramic matrix to meet the particular prerequisites including high thermal shock resistance, high hardness, non-magnetic and nonconductive properties [1–3,8]. Table 1.3. is a summary of the different heat exchangers and their characteristic features [3,10,11].

Table 1.3. continue

Types	Features							
	Compactness (m^2/m^3)	Stream types[1]	Materiel[2]	Temperature range (°C)	Max-pressure (bar)	Cleaning methods	Corrosion resistance	Multistram /multipass capacity
Diffusion-bonded plate-fin	700 up to 800	Gases, liquids, two –phase	Ti, s/s	up to 500	>200	Chemical	Excellent	Yes/Yes
Printed- Circuit	200 up to 5000	Gases, liquids, two –phase	s/s, Ni, Ni alloy, Ti	-200 up to +900	>400	Chemical	Excellent	Yes/Yes
Polymer (e.g. channel plate)	450	Gas-liquid[16]	PVDF[17], PP[18]	up to 150	6	Water wash	Excellent	No/Not usually
Plate-and-shell	--	liquids	s/s, Ti, (shell also in c/s)[20]	up to 350	70	Mechanical[4,15], Chemical[21]	Good	No/Yes
Marbond	<= 10000	Gases, liquids, two –phase	s/s, Ni, Ni alloy, Ti	-200 up to +900	>900	Chemical	Excellent	Yes/Yes

1.3.7. Factors that determine the choice among the three types of CHEs.

1. Operating pressure and temperature.
2. Phases of the fluids dealt with.
3. Fouling characteristics of the fluids.
4. Allowable Pressure Drop.
5. Strength and ruggedness.

6. Restrictions on size and/or weight.
7. Acceptable intermixing of the fluids dealt with.

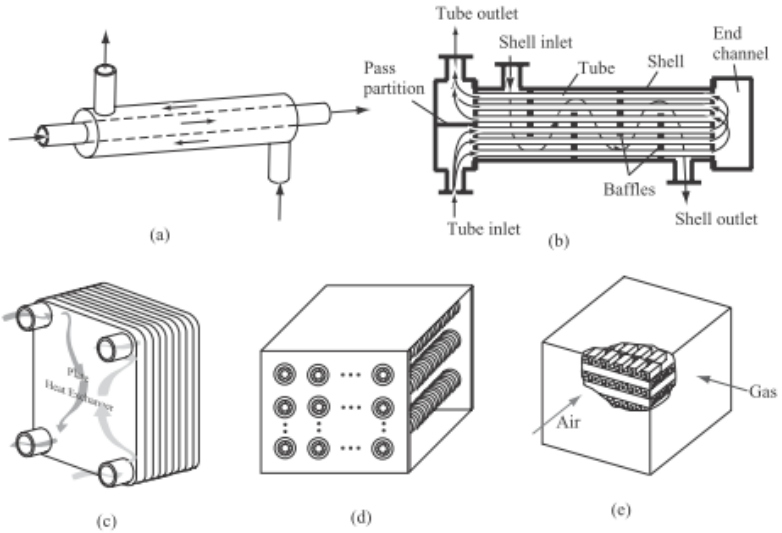

Figure 1.9. Typical heat exchangers: (a) double-pipe heat exchanger, (b) shell-and-tube heat exchanger, (c) brazed plate heat exchanger, (d) circular finned-tube heat exchanger, and (e) plate-fin heat exchanger (OSF) [12].

1.3.8. Advantages of compact heat exchangers over the other types of heat exchangers

1. Flexibility in disseminating surface area on the hot and cold sides as required by design requirements.
2. Generally light cost, weight, or volume savings.
3. Many surfaces are accessible having various degrees of magnitudes of surface density.

Figure 1.10. Complete Compact Heat Exchanger with manifolds [13].

1.4. Problem statement and objective of study

A gas turbine is classified as a continuous combustion internal combustion engine. Small scale gas turbines are gas turbines with an output of up to 500KW. These internal combustion engines unlike the traditional Otto and Diesel engines, work following the Brayton cycle. For these engines to achieve high efficiencies values of about 90%, with an electrical efficiency of about 35%, they need to be run with a recuperated energy cycle of varying configurations. Thus, the objective of this work is to design a heat exchanger for a small-scale gas turbine.

The main objective of this study is to design and run analytical studies on a heat exchanger system that will increase the efficiency of a small-scale gas turbine. The design of this heat exchanger will be based on an already existing gas turbine and its

working conditions. All the heat exchanger input data and assumptions were made with regards to this gas turbine. Figure 1.5 below presents the gas turbine and its features [14].

Figure 1.11. Small-scale gas turbine [14].

1. Turbo charging unit (1),
2. Combustion chamber and flame tube (2),
3. Exhaust system (3),
4. Ignition transformer (4),
5. Spark plug (5),
6. Injector pipe and injector (6),
7. Fuel tank (7),
8. Oil pump and lubrication system (8),
9. Fuel pump (9),
10. Secondary burning (after burning) system ignition transformer (10),
11. Secondary spark plug (11) after ignition system (11),
12. Load sensor (12),
13. Temperature and pressure display panel (13),

14. Push force indicator (14),
15. Combustion pressure gauge manometer (15),
16. Electric control box (16),
17. Fuel pump drive motor (17),
18. Secondary combustion fuel pump (18).

Table 1.4. Characteristics of gas turbine.

Combustion pressure: 33 kPa		
	Turbine	**Compressor**
Inlet temperature (˚C)	407	25
Outlet temperature (˚C)	525	49

CHAPTER 2 . LITERATURE REVIEW

2.1. Heat Exchangers Review

The area of heat exchangers has been of great interest among researchers for a long period of time now and several approaches have been taken in the design of heat exchangers that will serve certain purposes and respect certain conditions. These studies go as early as 1964, in early attempt, they carried out analytical solutions of the Nusselt Number for a large collection of duct shapes under laminar flow [15], where they used either constant wall temperature or constant wall heat flux boundary conditions and applying various techniques such as conformal mapping (Sastry 1964, 1965) and the Galerkin integral methods (Haji-heikh et al 1983) . A lot of surface geometry enhancement techniques for heat exchangers have also been proposed along the years. Heat exchanger surface geometries and fabrication techniques, together with specific recuperator sizes for different applications, has been presented [16]. In this work, he gave a detailed discussion on the design, performance, structural, manufacturing, and economic aspects of compact heat exchanger technology, as applied to the gas turbine, together with projected future trends. He also gave a broad use and advancement techniques applied in heat exchanger technology in the early years.

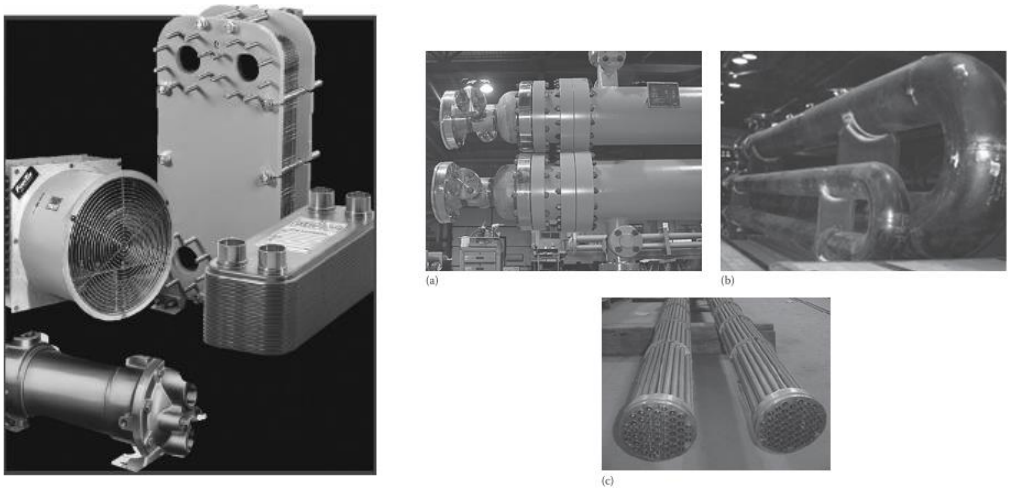

(i) (ii)

Figure 2.1. (i) Collection of few types of heat exchangers. (Courtesy of ITT STANDARD, Cheektowaga, NY.) (ii) Hairpin heat exchanger. (a) Separated head closure using separate bolting on shell-side and tube-side and (b) Hairpin exchangers for high-pressure and high temperatures [2].

Much work has also been covered on the different types of heat exchangers used in gas turbine units, the trend of research and development, and the need for future research [17]. In recent years, the application of heat exchangers and more especially compact heat exchangers has gained more grounds in aero engines. They evaluated the potential of heat exchanged aero engines for future Unmanned Aerial Vehicles (UAV), helicopters, and aircraft propulsion, with emphasis placed on reduced emissions, lower fuel burn and less noise [16,18]. Ji Hwang Jeong et al, (2009) suggested potential heat exchanger designs for an aero gas turbine recuperator, intercooler, and cooling-air cooler [19]. In power plants, Hossin Omar et al (2017), investigated the effects of regeneration on the output power and thermal efficiency of the gas turbine power plant. They also investigated the effects of ambient air temperature, regeneration effectiveness, and compression ratio on the cycle thermal efficiency. They based their investigations on an existing gas turbine power plant which is called AL ZAWIA [20].

2.2. Compact Heat Exchangers (CHEs) Review

Due to the need for light-weight, space-saving, and low cost, compact heat exchangers have gained more interest within the past years especially in gas turbine power plants, aircraft engines, micro gas turbines, cryogenics, ocean thermal energy conservation, solar and in situations where space is a constraint. As a result, there have been many studies carried out in this area. Picon-Nunez et al (1998), presented a methodology for the design of compact plate-fin heat exchangers where full pressure drop utilisation is taken as a design objective. Their methodology was based on the development of a thermo-hydraulic model that represent the relationship between pressure drop, heat transfer coefficient, and exchange volume. They also presented an approach to surface selection based on the concept of Volume Performance Index [21]. Utrianian et al (1998) also attempted to achieve compact heat exchangers for different applications and the application of CFD on specific recuperators. Southall et al (2008) discussed the design and surface enhancement considerations that lead to the optimal heat exchanger design. They laid special emphasis on the heat versus pressure drop performance considerations for enhanced surfaces [22]. Sunden (2010), presented some methods to analyse and determine the performance of compact heat exchangers; showed the applicability of various computational approaches and their limitations, provided examples to demonstrate the methods and presented results to highlight the opportunities and limitations of the considered method [5]. Berrin et al (2013), presented a comprehensive guide of compact heat exchangers; The finned surface arrangements; The working pressures and temperatures and sizes of plate-fin heat exchangers; fouling; thermal analysis. Alexander et al (2014) presented an alternative approach for the control of compact heat exchangers which can be implemented without the knowledge of the transfer behaviour and this method is robust against changes in the coolant supply system. To achieve this, they presented a model-based control strategy which relies on the total thermal energy stored in the fluids of the heat exchanger as control variable instead of the outlet temperature.

2.3. Advancements in CHE technology

Throughout the years, compact heat exchangers have witnessed continuous improvements. There have been a lot of advances in the theory, design, analysis, optimisation, and manufacturing technology of CHEs. These advances have mostly been done the areas of [23]:

a. Advances in two-fluid exchanger effectiveness and NTU results for highly complex flow arrangements,
b. Heat transfer and pressure drop analyses,
c. The role of CFD in the design and analysis of header and manifold design,
d. Recuperator design procedure,
e. Design data for compact heat exchangers,
f. Thermodynamic modelling and analysis,
g. Brazing of compact heat exchangers, and
h. Advancement in CHEs for new applications such as fuel cells and microturbines.

The automotive industry has also witnessed a considerable amount of progress in the design of CHEs. This is due to the need for a reduction in the cost and space of these exchangers. This has led to a continuous reduction in the size of automotive evaporators and condensers. The Figure 2.2 below shows the evolutionary progress in the size of these condensers. Another sector that has experienced this advancements is the air conditioning sector [10]. In order to well understand the heat characteristics, properties and flow means of these CHEs a lot of work has been carried out in the following areas[3]; flow visualisation [4,24–26], heat transfer and pressure drop measurement [27–29] and numerical simulation [25,30].

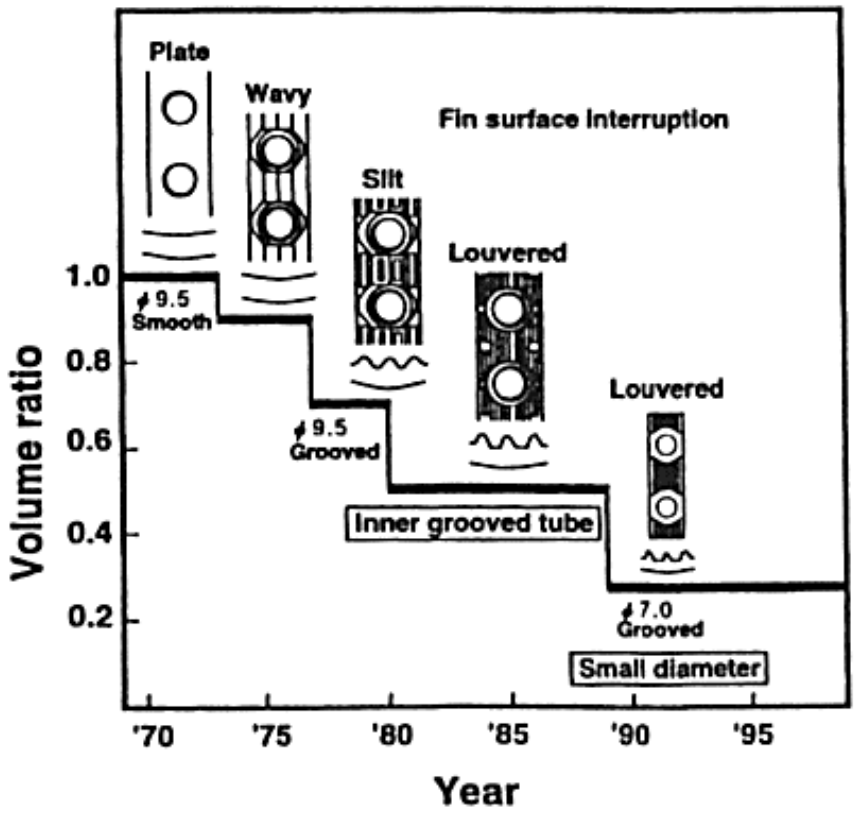

Figure 2.2. Progress in air conditioning condenser technology, showing simultaneous air side and refrigerant side improvements [10].

Also, Rolls Laval Heat Exchangers Ltd. applied a cost effective technique in the construction of PFHEs which they developed from the manufacturing of their aero-engine parts. They applied the procedure of diffusion bonding and then super plastically forming (SPF/DB). This allowed them to make a complete reach of internal geometries except for conventional fin arrangements and perforated variants[3,8]. It has an area density of 700–800 m^2/m^3. The bond strength of the SPF/DB core is that of the parent metal, and very high containment pressures can be sustained. Nonetheless, the porosity is like those of the brazed PFHE, generally about 0.6–0.75 [40]. Typical channel heights are about 2–5mm[3,8,10].

2.4. Application of Compact Heat Exchangers in Gas Turbines

In a thermodynamic cycle of any heat engine, there is the addition of heat from a heat source to a working medium and the rejection of the used heat to a heat sump or environment. The gas turbine is a complex cycle which involves heat sources and sumps that work simultaneously in some of the cases. The heat source can be a burning fuel or an external source through a heat exchanger or both. Meanwhile, the heat rejection from hot working medium takes place through the exhaust gas to the ambient atmosphere or to the heat tank or heat exchanger. During the past years in order to increase the efficiency of gas turbines and to abide to the different emissions regulations, researchers have worked on the improvement of these heat sources. One of the core approaches which researchers have used to provide a solution to this problem is the recuperation or regeneration of the gas turbine's exhaust gas heat. This is done through the use of a heat exchanger unit which is placed between the exhaust unit and the combustion chamber.

Due to the need for lightweight, space-saving, and economic factors, the Compact Heat Exchanger has been used in wide variety of applications of gas turbines. Typical among these are gas turbines used in automobiles, cryogenics, aircraft and spacecraft, ocean power plants, and small-scale or micro gas turbines. Below is a thermodynamic cycle and a scheme of a typical gas turbine [2,31,32], [1].

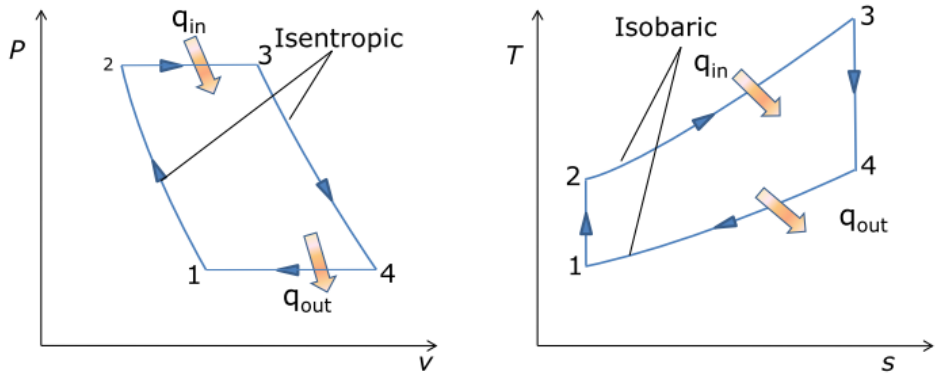

Figure 2.3. The typical gas turbine cycle- the Brayton Cycle.

The typical gas turbine operates under the Brayton Cycle. The Brayton cycle consists of four internally reversible processes:

a. 1-2 Isentropic compression (in a compressor)
b. 2-3 Constant-pressure heat addition
c. 3-4 Isentropic expansion (in a turbine)
d. 4-1 Constant-pressure heat rejection

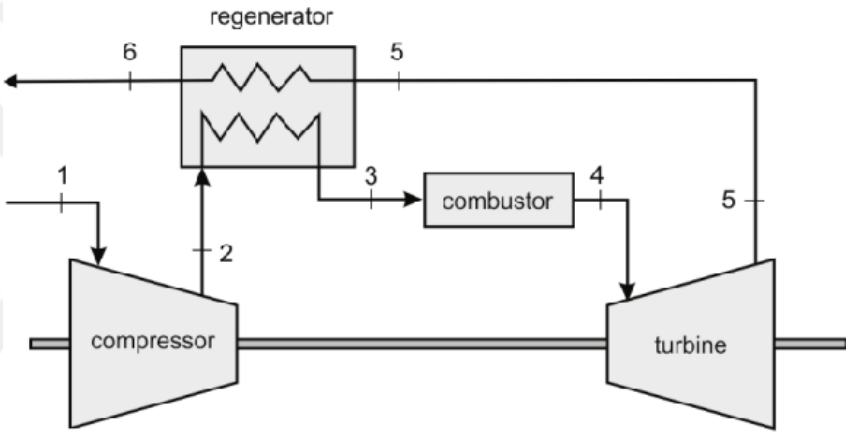

Figure 2.4. A typical open gas turbine scheme

The thermal efficiency of the Brayton cycle (Gas turbine cycle) is as follows

$$\eta_{th,Brayton} = 1 - \frac{1}{\beta^{\frac{k-1}{k}}} \tag{2.1}$$

Where, $\beta = \frac{P_2}{P_1}$, is the pressure ratio.

Also $\left(\frac{P_2}{P_1}\right)^{\frac{(k-1)}{k}} = \frac{T_1}{T_2}$

The thermal efficiency of a Brayton cycle is, therefore, a function of the cycle *pressure ratio* and the *ratio of specific heats*. Thus, to improve on the thermal efficiency of the gas turbine one must work on the different pressures or temperatures.

2.4.1. Brayton cycle with regeneration or gas turbine cycle with heat exchanger

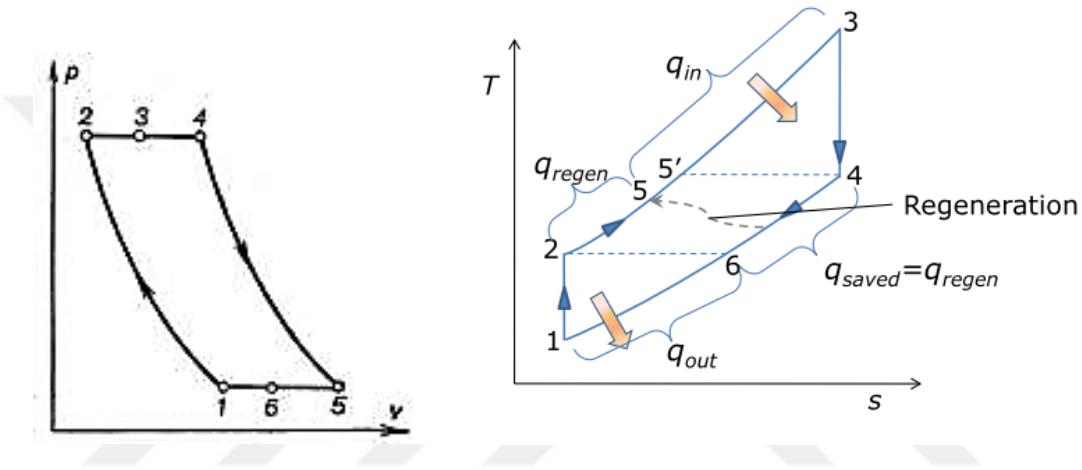

Figure 2.5. Gas turbine cycle with heat exchanger

Here, the working medium or inlet air is compressed in the compressor through a multi-step process (1-2), the compressed air is heated up by heat which is extracted from the heat of the exhaust gases through a regenerator which will be our CHE (2-3), the preheated air is further heated up in the combustion chamber by a burning fuel (3-4), the combusted air then expands in the turbine (4-5), this rejected air is then cooled in the heat exchanger where some of its heat is extracted (5-6) and lastly the waste air is rejected into the ambient air for an open cycle. In the case of a closed cycle, this air is recollected through the compressor inlet (6-1).

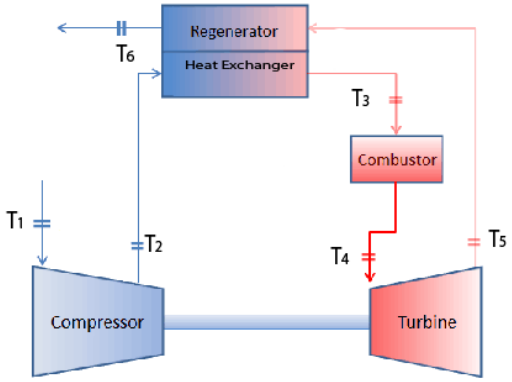

Figure 2.6. Gas turbine with heat exchanger scheme

2.4.2. Thermal efficiency of gas turbine cycle with heat exchanger

a. Regenerative cycle of a constant-pressure gas turbine with isothermal air compression

Let's consider the cycle below [31]

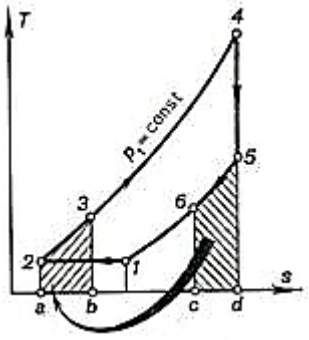

Figure 2.7. Constant pressure gas turbine with isothermal air compression.

The heat added into the cycle

$$q_1 = c_p(T_4 - T_3) \tag{2.2}$$

And the rejected heat is

$$q_2 = RT_1 \ln\frac{P_2}{P_1} + c_p(T_6 - T_1) \tag{2.3}$$

This can further be written as

$$q_2 = RT_1 \ln\frac{P_2}{P_1} + c_p(T_5 - T_1) - c_p(T_3 - T_2) \tag{2.4}$$

The thermal efficiency can now be determined as

$$\eta_{Brayton,regen} = 1 - \frac{q_2}{q_1} \tag{2.5}$$

$$\eta_{Brayton,regen} = 1 - \frac{\frac{k-1}{k}\ln\beta}{\gamma(\rho - 1)} + \frac{\beta^{\frac{k-1}{k}} - \rho}{\beta^{\frac{k-1}{k}}(\rho - 1)} \tag{2.6}$$

Where,

$$\rho = \frac{v_4}{v_3} = \frac{T_4}{T_3}, \frac{P_2}{P_1} = \beta, \frac{T_3}{T_2} = \gamma \tag{2.7}$$

Then

$$\frac{T_5}{T_2} = \frac{T_5}{T_4}\frac{T_4}{T_3}\frac{T_3}{T_2} = \left(\frac{P_5}{P_4}\right)^{\frac{k-1}{k}} \rho\gamma = \left(\frac{P_1}{P_2}\right)^{\frac{k-1}{k}} \rho\gamma = \frac{\rho\gamma}{\rho^{\frac{k-1}{k}}} \quad (2.8)$$

It follows that the greater γ is (γ characterizes the degree of regeneration**),** the higher is the thermal efficiency of a constant-pressure combustion gas-turbine. With a maximum degree of regeneration, σ = 1 and, consequently, $\gamma_{max} = T_5/T_2 = T_5/T_1$. All the heat available in the exhaust gases is then utilized to heat the compressed air. Such regeneration is referred to as complete. This case is only of theoretical importance since, at a zero-temperature difference between the exhaust gases and air, which would have taken place in the event of complete regeneration, no heat transfer is possible in heat exchanger. In this case at $T_3 = T_5$ the degree of preliminary expansion will be:

$$\rho = \frac{V_4}{V_3} = \frac{T_4}{T_5} = \left(\frac{P_4}{P_5}\right)^{\frac{k-1}{k}} = \beta^{\frac{k-1}{k}} \quad (2.9)$$

Substituting this into our equation for efficiency, we get

$$\eta_{Brayt,regen,max} = 1 - \frac{\frac{k-1}{k} T_1 \ln \beta}{T_5\left(\beta^{\frac{k-1}{k}} - 1\right)} \quad (2.10)$$

The higher the temperature T_5, the higher the thermal efficiency of the cycle. The expression shows the necessity of raising the temperature T_5 at the end of expansion which unfortunately is hampered due to the comparatively low mechanical strength of the materials of gas-turbine blades at high temperatures.

b. Regenerative cycle of a constant-pressure gas turbine with adiabatic air compression

Let's consider the cycle below [31].

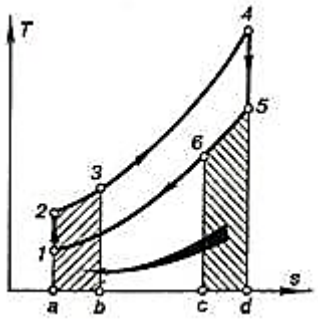

Figure 2.8. Constant pressure gas turbine with adiabatic air compression

The added heat is

$$q_1 = c_p(T_4 - T_3) \tag{2.11}$$

The rejected heat is

$$q_2 = c_p(T_6 - T_1) = c_p(T_5 - T_1) - c_p(T_5 - T_6) \tag{2.12}$$

But

$$c_p(T_5 - T_6) = c_p(T_3 - T_2) \tag{2.13}$$

Which implies

$$q_2 = c_p(T_5 - T_1) - c_p(T_3 - T_2) \tag{2.14}$$

The thermal efficiency of the cycle will then be

$$\eta_{Brayton,regen} = 1 - \frac{c_p(T_5 - T_1) - c_p(T_3 - T_2)}{c_p(T_4 - T_3)} \tag{2.15}$$

Expressing in terms of the ratios, we get

$$\eta_{Brayton,regen} = 1 - \frac{(\rho\gamma - 1) - \beta^{\frac{k-1}{k}}(\gamma - 1)}{\gamma\beta^{\frac{k-1}{k}}(\rho - 1)} \tag{2.16}$$

Where

$$\frac{T_2}{T_1} = \left(\frac{p_2}{p_1}\right)^{\frac{k-1}{k}} = \beta^{\frac{k-1}{k}}, \frac{T_4}{T_5} = \left(\frac{p_4}{p_5}\right)^{\frac{k-1}{k}} = \beta^{\frac{k-1}{k}} \tag{2.17}$$

Thus

$$\frac{T_5}{T_1} = \frac{T_4}{T_2} = \frac{T_4}{T_3}\frac{T_3}{T_2} = \rho\gamma,$$

$$\frac{T_3}{T_1} = \frac{T_3}{T_2}\frac{T_2}{T_1} = \gamma\beta^{\frac{k-1}{k}}, \quad \frac{T_4}{T_1} = \frac{T_4}{T_3}\frac{T_3}{T_2}\frac{T_2}{T_1} = \rho\gamma\beta^{\frac{k-1}{k}}. \tag{2.18}$$

The maximum possible degree of regeneration or regeneration fraction occurs at $T_3 = T_5$, i.e. at $\gamma_{max} = T_5/T_2$. In this case

$$\frac{T_5}{T_1} = \frac{T_3}{T_1}$$

And

$$\frac{T_4}{T_1} = \frac{T_4}{T_5}\frac{T_5}{T_1} = \beta^{\frac{k-1}{k}}\gamma_{\max}\beta^{\frac{k-1}{k}}. \quad (2.19)$$

Thus, we have the maximum efficiency as

$$\eta_{Brayt,regen,max} = 1 - \frac{1}{\gamma_{max}\beta^{\frac{k-1}{k}}} \quad (2.20)$$

But

$$\gamma_{\max} = \frac{T_3}{T_2} = \frac{T_3}{T_1}\frac{T_1}{T_2} = \frac{T_5}{T_1}\frac{1}{\beta^{\frac{k-1}{k}}}; \quad (2.21)$$

Thus,

$$\eta_{Brayt,regen,max} = 1 - \frac{T_1}{T_5} \quad (2.22)$$

Thus, the thermal efficiency of a constant-pressure gas-turbine operating with maximum regeneration and adiabatic compression depends only on the temperature of the gas at the end of adiabatic expansion, T_5.

2.4.3. Comparison between constant-pressure gas turbine with isothermal air compression and constant-pressure gas turbine with adiabatic air compression

Normally both cycles are being carried out or realised at different initial temperatures and pressure but at the same maximum temperature. From the figure below [31]

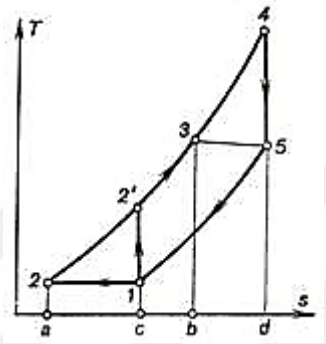

Figure 2.9. Isothermal and Adiabatic Compressions of a Gas Turbine with Heat Exchanger

The thermal efficiency of the cycle with isothermal compression and complete heat regeneration

$$\eta_{max} = \frac{l_c}{q_1} = \frac{area\ (1-2-4-5-1)}{area\ (b-3-4-d-b')} \tag{2.23}$$

and the thermal efficiency of the cycle with adiabatic compression and maximum heat regeneration

$$\eta'_{max} = \frac{l_c}{q_1} = \frac{area\ (1-2'-4-5-1)}{area\ (b-3-4-d-b')} \tag{2.24}$$

We can see that the energy source in both cases is the same, but they have different energy outputs. It's clear that the cycle with Isothermal compression is more efficient

than the cycle with Adiabatic compression with both having the same maximum temperature.

CHAPTER 3 . MATERIALS AND METHODS

In this work, we adopted the design methodology (Figure 3.1.) as proposed by Shah and Sekulic [33] with slight modifications. Firstly, the design specifications will be determined, then the design calculations will done following the algorithm proposed by Shah, [33]. From this calculation, the heat exchanger dimensions will be determined. The next phase will be to come out with a 3D representation of the heat exchanger using a CAD tool (SOLIDWORKS). Then simulations and heat flow analysis will be carried out using SOLIDWORKS Flow Simulation.

3.1. Materials

Plate-fin heat exchangers are by and large, produced using a combination of aluminium or stainless steel. Be that as it may, the procedure temperature and weight direct the decision of the material. Aluminium alloys are especially reasonable for low-temperature applications in view of their low weight and phenomenal pliability and expanding quality under such conditions. All in all, the fins or secondary surfaces and the sidebars are generally joined to the isolating plate by utilizing plunge brazing innovation or all the more as of late vacuum brazing strategy. The brazing material in the event of aluminium exchangers is an aluminium alloy of lower dissolving point, while that utilized in stainless steel exchangers is a nickel-based composite with proper liquefying and welding qualities [34].

3.2. Plate Fin Heat Exchanger Manufacturing Methods

The essential standards of plate-fin heat exchanger assembling are independent of the sizes and all materials used; sheets and ridged fins in a sandwich arrangement. Isolating plates (for example separating sheets) give the essential heat transfer surface.

Isolating plates are situated alternately with the layers of fins in the stack to frame the control between individual layers [34]. The separating plates are produced using one of the following methods [13];

a. Mechanical forming, where a metal coil is passed through a fin press to form corrugated channels that are approximately rectangular.
b. Photochemical etching, where material is removed from flat metal sheets to form channels that are approximately semi-circular.

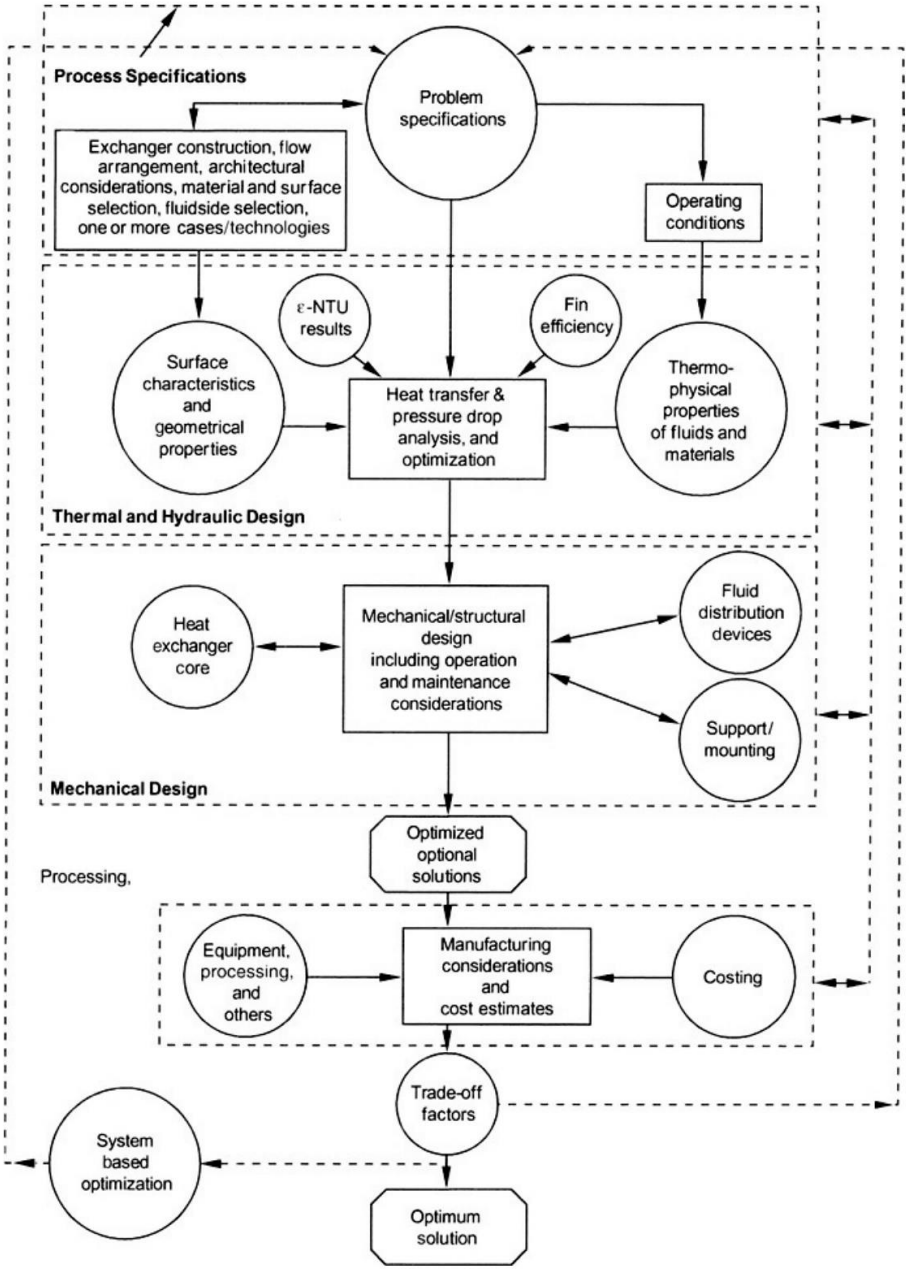

Figure 3.1. Compact heat exchanger design methodology [33].

These components, for example, the corrugations, sidebars, parting sheets, and cap sheets are then held together in an equip under a predefined load, and put in a heater and brazed to produce the plate-fin heat exchanger block. After this the header tanks and spouts are welded to the block, taking consideration that the brazed joints stay flawless during the welding procedure. Contrasts emerge in the way through which the brazing procedure is done.

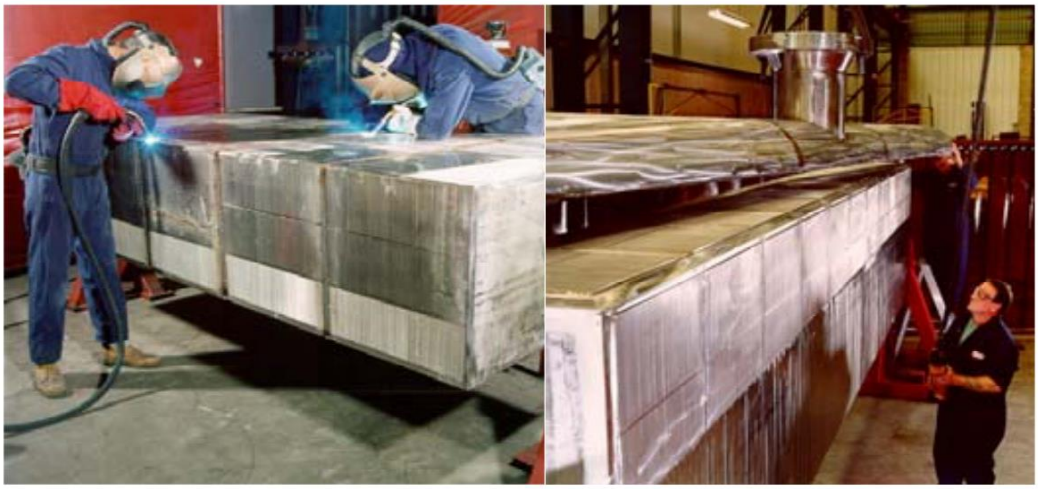

Figure 3.2. The manufacturing process of PFCHEs [13]

The techniques mostly applied are salt bath brazing and vacuum brazing. In the salt bath process, the stacked parts are preheated in a heater to around 5500 ^{o}C and after that plunged into a bath of melded salt made for the most part out of fluorides or chlorides of soluble base (alkali) metals [34]. The liquid salt fills in as both transition and heating agent, keeping up the furnace at a uniform temperature. Concerning heat exchangers made up of aluminium, the liquid salt evacuates oil/grease and the steady layer of aluminium oxide, which would somehow debilitate the joints. Brazing happens in the bath when the temperature is raised above the melting point of the brazing alloy. The brazed block is purified of the remaining hardened salt by dissolving in water and is then completely dried. [13,34]

During the vacuum brazing process, no flow or separate pre-warming heater is required. The built block is heated to brazing temperature by radiation from electric radiators and by conduction from the outside surfaces into the inside of the block. The exclusion of oxygen in the brazing milieu is guaranteed by the use of a high vacuum pump (Pressure ≈ 10-6 Mbar). The content of the remaining gas is additionally improved (lower oxygen content) by evacuation and refilling up with an inactive gas as much as experience directs. No washing or drying of the brazed block is needed.

Numerous metals, for example, aluminium, tempered steel, copper and nickel amalgams can be brazed successfully in a vacuum furnace. [13,34].

3.3. Factors That Influence the Design and Manufacturing of Plate-Fin Compact Heat Exchangers

Prior to beginning the designing of the heat exchanger, the necessities of the proposed heat exchanger power and characteristics are screened to check for attainability. This underlying screening should answer following questions as defined by David S. et al [35].

a. Design pressure and temperature.
b. Process fluids.
c. Heating/cooling curves.
d. Allowable pressure drop.
e. Required thermal effectiveness.

3.4. Problem Specification

Design specifications: Due to the operating fluids all being gases, low cost, low space requirements, manufacturability, and operating temperatures and pressures, the regenerator will be of the Plate-Fin Compact Heat Exchanger (PFCHE) type with Rectangular fins and a crossflow arrangement.

1. Required Effectiveness: $\varepsilon = 0.8381$.
2. Fin height: $b_h = b_c = 15mm$
3. Fin thickness: $\delta_w = 1mm$, $\delta_h = \delta_c = \delta_w$
4. Heat transfer surface area density: $\beta_c = \beta_h = 2000m^2/m^3$
5. Fin area/total area ratio: $\left(\frac{A_f}{A}\right)_h = \left(\frac{A_f}{A}\right)_c = 0.785$
6. Hydraulic diameter: $D_{h,h} = D_{h,c} = 1.6mm$
7. Fluid mass flow rates: $\dot{m}_h = 1.66kg/s$, $\dot{m}_c = 2.0kg/s$

8. Pressure drop : $\Delta P_h = 9.0kPa$, $\Delta P_c = 8.79kPa$
9. Plate Thermal heat transfer (Both plates are made of steel): $k_w = 33\ W/mK$
10. Inlet Temperatures of gases: $T_{h,i} = 798K,\ T_{c,i} = 317K$

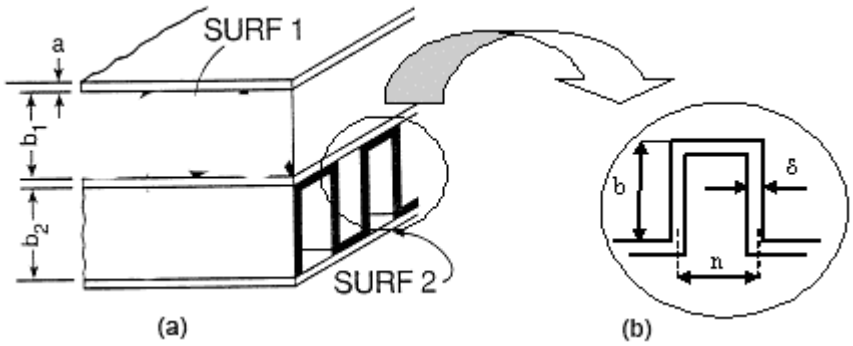

Figure 3.3. Definition of Fin Geometric Terms

3.5. Heat Transfer and Hydraulic Flow analysis

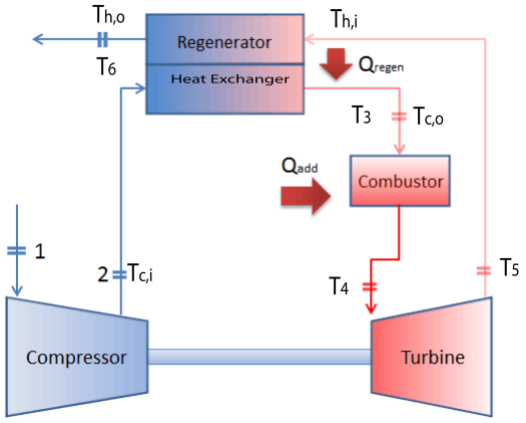

Figure 3.4. Gas Turbine with Heat Exchanger Flow Diagram

3.5.1. Outlet temperatures ($T_{i,o}$)

Assuming the same heat capacity for both the hot and cold streams of air, we have [33], for the hot gas outlet temperature

$$T_{h,o} = T_{h,i} - \varepsilon\left(T_{h,i} - T_{c,i}\right) \quad (3.1)$$

Where, ε is the effectiveness value which is a measure of the thermal performance of a heat exchanger. Its expressed as the ratio between the actual heat transfer rate and the maximum heat transfer rate.

Substituting the values give,

$T_{h,o} = 394.87K$

And for the cold air we have,

$$T_{c,o} = T_{c,i} + \varepsilon\frac{\dot{m}_h}{\dot{m}_c}\left(T_{h,i} - T_{c,i}\right) \quad (3.2)$$

$\dot{m}_x$ is the fluid mass flow rate.

Thus giving,

$T_{c,o} = 651.59K.$

This value will be recalculated after the fluid properties have been determined.

3.5.2. The fluid properties

Arithmetic Mean Temperature (AMT): This is the average temperature of the gases. The fluid properties are will be assessed at this temperature.

For the hot stream we get,

$$T_{h,m} = \frac{T_{h,i} + T_{h,o}}{2} = 596.44K \quad (3.3)$$

And for the cold stream we have

$$T_{c,m} = \frac{T_{c,i} + T_{c,o}}{2} = 484.3K \tag{3.4}$$

From the above mean temperature value, we have the following specific heats,

$$c_p(T_{h,m}) = 1.051\ kJ/kgK$$

$$c_p(T_{c,m}) = 1.030\ kJ/kgK$$

The corrected value of the cold stream outlet temperature can now be gotten as,

$$T_{c,o} = T_{c,i} + \varepsilon\left(\frac{\dot{m}_h c_{p,h}}{\dot{m}_c c_{p,c}}\right)(T_{h,i} - T_{c,i}) \tag{3.5}$$

Putting in the respective values give,

$$T_{c,o} = 658.42\ K$$

Refined value of Cold stream AMT

$$T_{c,m} = \frac{T_{c,o} + T_{c,i}}{2} = 487.71K \tag{3.6}$$

Table 3.1. Summary of fluid properties.

	$\mu(10^3\ Pa.s)$	c_p(kJ/kgK)	P_r	$P_r^{2/3}$
Hot air stream ($T_{h,m}$)	305.8	1.051	0.685	0.777
Cold air stream ($T_{c,m}$)	270.1	1.030	0.684	0.776

Table 3.2. Summary of Densities.

	$T_i(k)$	$T_o(k)$	$\rho_i(kgm^3)$	$\rho_o(kgm^3)$	$\rho_m(kgm^3)$
Hot air stream	798	394.87	0.4354	0.8711	0.5804
Cold air stream	317	658.42	1.1614	0.5356	0.6964

3.5.3. The Number of Transfer Units (NTU)

The NTU is the ratio of the overall thermal conductance to the smaller heat capacity rate. The NTU is used to calculate the rate of heat transfer of a heat exchanger when there is insufficient information to use the Log-Mean Temperature Difference (LMTD) like in this our case. From the fluid properties, we have the following heat capacity values,

$$C_h = \left(\dot{m}c_p\right)_h = 1.745\ kW/K$$

$$C_c = \left(\dot{m}c_p\right)_c = 2.06\ kW/K \tag{3.7}$$

Thus,

$$C_r(C^*) = \frac{C_{min}}{C_{max}} = 0.847 \tag{3.8}$$

From the problem specifications we had $\varepsilon = 0.8381$, and with above value of C_r and referring to figure below, we have

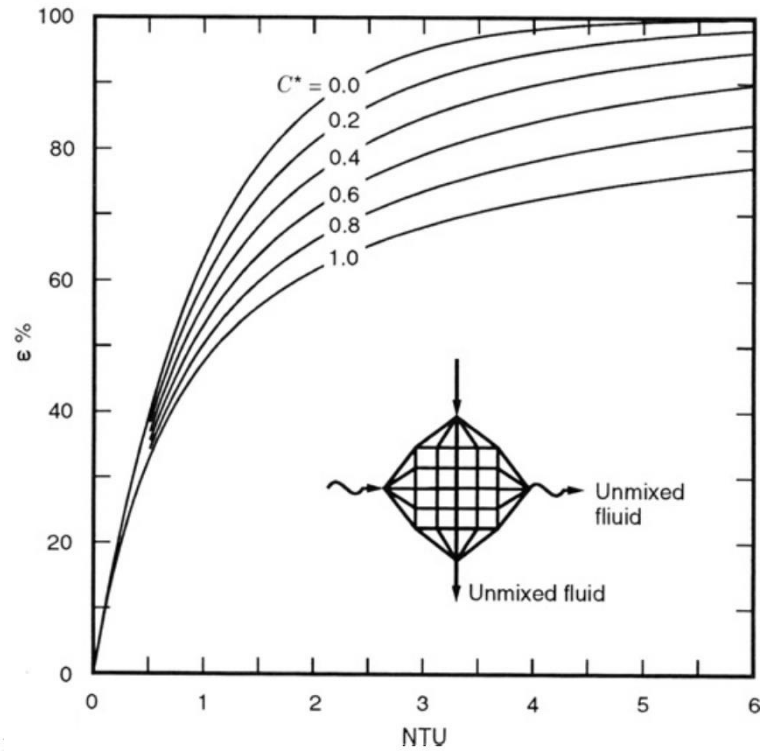

Figure 3.5. Unmixed-unmixed crossflow exchanger E as a function of NTU and C* [33]

$NTU = 5.395$ (this is the overall NTU for the heat exchanger)

For our gas-to-gas HE and assuming a thermally balanced design and no thermal wall resistance, we get [33]

$$ntu_h = 2NTU = 10.790 \quad (3.9a)$$

$$ntu_c = 2C_r NTU = 9.139 \quad (3.9b)$$

These *ntu* values permit us to determine the core mass velocities of the fluids in the different flow streams as seen in equation 3.10.

3.5.4. Core mass velocities (G)

The core mass velocity G relates the fluid flow velocity to the flow rate of the fluid. For G to be calculate, the j/f factor is required. The *j/f* factor is a heat exchanger surface performance characterisation parameter. It is applied for heat exchangers with Prandtl number different from unity. Also, it is required for the evaluation of G and in order to evaluate *j/f*, we need the Reynolds number, which cannot be calculated now. Thus, based on the known data, an approximate average (‘‘ballpark’’) value of *j/f* over the complete range of Re is taken for each surface from the figure 3.13. below as. [10,33]

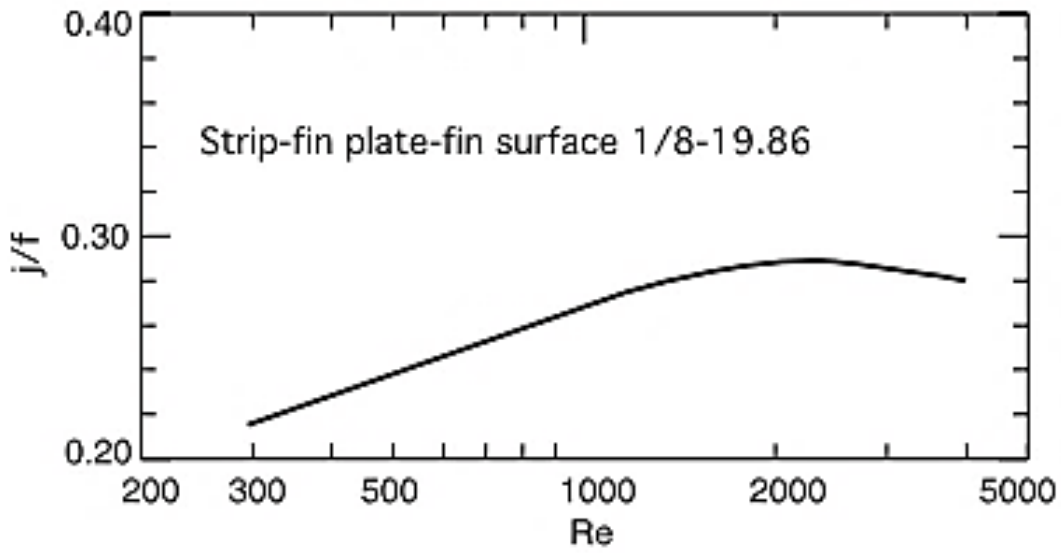

Figure 3.6. *j/f* vs. Re characteristics of surfaces [33]

$(j/f)_h \approx 0.25$, $(j/f)_c \approx 0.25$ and we will assume $\eta_0 = 0.8$

From the above approximates, G is thus gotten as follows [33]

$$G_i = \left[\frac{2g_c}{\left(\frac{1}{\rho}\right)_m P_r^{2/3}} \frac{\eta_0 \Delta P}{ntu} j/f \right]_i^{1/2} \quad (3.10)$$

Where, $i = h, c$

Putting in the values give

$G_h = 6.3047\ kg/m^2s$ and $G_c = 7.0153\ kg/m^2s$

3.5.5. Reynolds number (Re) and *j* (Colburn factor), *f* (Fanning friction factor) factors

The Reynolds number is a fluid flow characterisation property. This value characterises whether a flow is laminar or turbulent. The Reynolds value for PFHE can be determined as follows [33].

$$Re_i = \left(\frac{GD_h}{\mu}\right)_i \quad (3.11)$$

Thus, $Re_h = 329.84$ and $Re_c = 415.57$, laminar flow since the value of Reynolds number is less than 2100.

j is the Colburn factor; it is a heat exchanger surface performance parameter that is applied in heat transfer characterisation of flow with Prandtl number different from unity. *f* is the fanning friction factor; it relates fluid flow mean velocity to the mass flow rate.

For plane rectangular PFHE and laminar flow [36], we have

$$f_i = 12.892 Re_i^{-1.229} \left(\frac{b}{n}\right)_i^{0.452} \left(\frac{\delta_w}{n}\right)_i^{-0.198} \quad (3.12)$$

And

$$j_i = 0.454 Re_i^{-0.977} \left(\frac{b}{n}\right)_i^{0.455} \left(\frac{\delta_w}{n}\right)_i^{-0.277} \quad (3.13)$$

Putting in the values gives,

	Re	j	f
Hot air stream	329.84	0.0358	0.01963
Cold air stream	415.57	0.02856	0.014777

3.5.6. Heat transfer coefficient

We have, [1,33]

$$h_i = \left(\frac{jGC_p}{P_r^{2/3}}\right)_i \quad (3.14)$$

Giving

$h_h = 305.3\ W/m^2K$ and $h_c = 265.94\ W/m^2K$

3.5.7. Fin efficiency (η_f)

The fin efficiency is expressed as follows [10,33]

$$\eta_{f,i} = \left(\frac{\tanh\,(ml)}{ml}\right)_i \tag{3.15}$$

Where,

$$m_i = \left[\frac{2h}{k_f \delta}\left(1 + \frac{\delta}{l_s}\right)\right]_i^{1/2} \tag{3.16}$$

Applying the data gives,

$m_h = 43.058\ m^{-1}$ and $m_c = 40.184\ m^{-1}$

Also

$$l_c = l_h = \frac{b}{2} - \delta = 0.0065m \tag{3.17}$$

Thus,

$\eta_{f,h} = 0.9747$ and $\eta_{f,c} = 0.9779$

3.5.8. Overall surface efficiency ($\boldsymbol{\eta_o}$)

The overall surface efficiency is determined as follows [33]

$$\eta_o = 1 - (1 - \eta_f)\frac{A_f}{A} \tag{3.18}$$

Which gives

$\eta_{o,h} = 0.980$ and $\eta_{o,c} = 0.983$

3.5.9. Overall heat transfer coefficient (*U*)

The overall heat transfer coefficient is evaluated as follows [1,10,37]. This value permits us to determine the rate at which heat will be transferred from one fluid to the other.

$$\frac{1}{U} = \frac{1}{(\eta_o h)_h} + \frac{\alpha_h/\alpha_c}{(\eta_o h)_c} \tag{3.19}$$

Where,

$$\alpha_i = \frac{(b\beta)_i}{b_c + b_h + 2\delta_w} \tag{3.20}$$

Where, β is the surface area per unit volume between parting sheets and b_c, b_h are the fin heights for the cold air stream and the hot gas stream passages respectively.

Putting in the values give

$\alpha_h = 1056.56\ m^2/m^3$ and $\alpha_c = 1056.56\ m^2/m^3$

Hence,

$$\frac{A_c}{A_h} = \frac{\alpha_c}{\alpha_h} = 1.0 \tag{3.21}$$

We then have

$U_h = 139.5\ W/m^2K$

3.6. Total surface area (A)

This is the total surface area in contact with the fluid. For the hot air stream, we have [10,33]

$$A_h = NTU\frac{C_h}{U_h} \tag{3.22}$$

Which gives

$A_h = 674.86\ m^2$

3.6.1. Minimum free flow area (Ao)

This is the open flow area on either of the fluid flow directions. For the free flow area, we have [10,33]

$$A_{o,h} = \left(\frac{\dot{m}}{G}\right)_h \tag{3.23}$$

Which gives, $A_{o,h} = 0.2635\ m^2$

3.6.2. Air flow length (L)

This is the length through which the fluid flows within the heat exchanger from the inlet end to the outlet end. The air flow length is expressed as follows [33]

$$L_h = \left(\frac{D_h A}{4A_o}\right)_h \tag{3.24}$$

Which gives, $L_h = 1.024\ m$

Since $\frac{A_c}{A_h} = 1.0$, we get

$A_c = 674.86\ m^2$

Thus, $A_{o,c} = 0.2851\ m^2$ and $L_c = 0.947\ m$

3.6.3. Core frontal area (A_{fr})

The core frontal area is expressed as follows. [33]

$$A_{fr} = \frac{A_o}{\sigma} \tag{3.25}$$

Where,

$$\sigma_i = \left(\frac{\alpha D_h}{4}\right)_i \tag{3.26}$$

But we have $\alpha_h = \alpha_c$, thus $\sigma_h = \sigma_c$

$\sigma_h = 0.423$

We then have

$A_{fr,h} = 0.6229\ m^2$ and $A_{fr,c} = 0.6740\ m^2$

But the frontal area can also be calculated from.

$$A_{fr} = L_1 L_2 \tag{3.27a}$$

Which implies,

$$A_{fr,h} = L_c L_3 \tag{3.27b}$$

Giving $L_3 = \frac{A_{fr,h}}{L_c} = 0.6578\ m$ or 0.6482 m

We then have the following dimensions.

	Calculated value (m)	Round-up value (mm)
L_h	1.024	1000
L_c	0.947	1000
L_3	0.648	650

3.7. Heat Transfer between Fluids

The effectiveness (***ε***) is defined as the ratio of the actual heat transfer rate and the maximum heat transfer rate. This is expressed as follows [1,10,38]

$$\varepsilon = \frac{Q}{Q_{max}} \tag{3.28}$$

The maximum heat transfer rate, Q_{max}, between the fluids can be determined from Equation 2.7 [1] as expressed below

$$Q_{max} = U_h A(T_{h,i} - T_{h,o}) \tag{3.29}$$

Thus, the actual heat transfer between the fluids is

$$Q = \varepsilon Q_{max} \tag{3.30}$$

3.8. Pressure Drop and Optimisation

From (Ramesh K. Shah & Dušan P. Sekulic, 2003, figure 6.3) [33], we got the following values for the entrance and exit loss coefficient

$k_{c,c} = k_{h,h} = 1.116$ and $k_{e,h} = k_{e,c} = 0.002371$

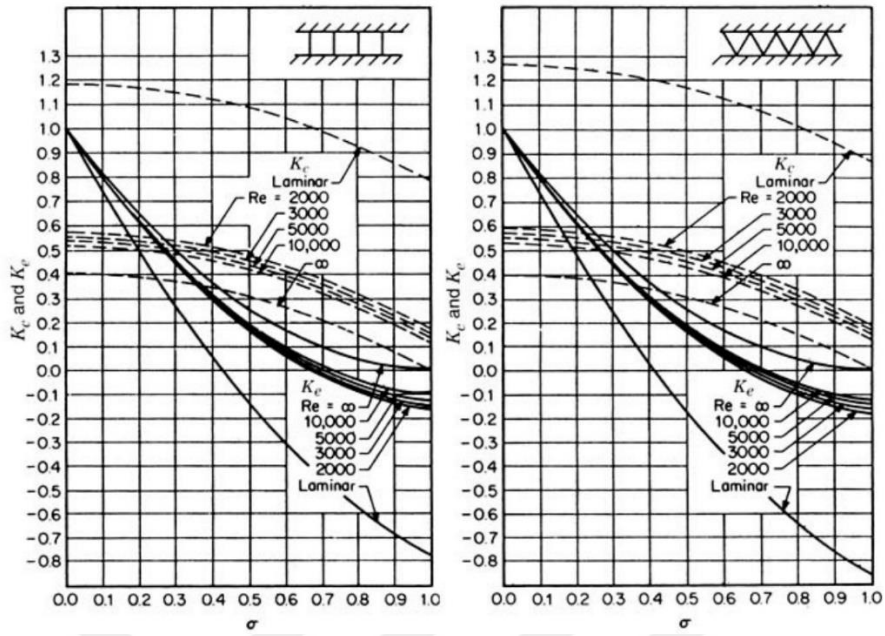

Figure 3.7. Entrance and exit pressure loss coefficients for multiple square tube core and multiple triangle tube core [33].

3.8.1. Thermal resistances (R)

We have [33]

$$R_i = \left(\frac{1}{\eta_o h A}\right)_i \tag{3.31}$$

Which gives,

$R_h = 4.954 * 10^{-5} K/W$ and, $R_c = 5.669 * 10^{-5} K/W$

And

$\frac{R_h}{R_c} = 1.144$

The wall Temperature is expressed as follows

$$T_w = \frac{T_{h,m} + (R_h/R_c)T_{c,m}}{1 + (R_h/R_c)} = 538.42\ K \tag{3.32}$$

3.8.2. Corrected fanning friction factor (*f*)

The corrected f factor is gotten from the following expression [33]

$$f_i = \left[f_{cp} \left(\frac{T_w}{T_m} \right)^n \right]_i \tag{3.33}$$

Taking $m = 0.81$ and $f_{cp} = 0.0695$, we have

$f_h = 0.0181$ and $f_c = 0.0163$

3.8.3. Pressure Drop ΔP

From [33] we have the expression of the pressure drop as follows,

$$\Delta P_i = \frac{G^2}{2g_c f_i} \left[(1 - \sigma^2 - k_c) + 2\left(\frac{\rho_i}{\rho_o} - 1 \right) + f \frac{L}{r_h} \rho_i \left(\frac{1}{\rho} \right)_m - (1 - \sigma^2 - k_e) \frac{\rho_i}{\rho_o} \right]_i \tag{3.34}$$

After the numerical application for both streams of air, we have the following results

$\Delta P_h = 1.509\ KPa$ and $\Delta P_c = 1.369\ KPa$

The values of the pressure drop are less than the ones previously assumed. Thus, they can be accepted. But in the case where a specified value is desired, the value of core velocity value (G) can be varied and the whole process repeated. This iteration will be repeated until the desired value is achieved.

From the obtained dimensions and properties of the PFCHE, we will now construct a 3-D model (figure 3.15) of the heat exchanger in SOLIDWORKS for the various tests and analysis. The full dimensions of the different components of the heat exchanger can be seen in Figures 4.1-4.5.

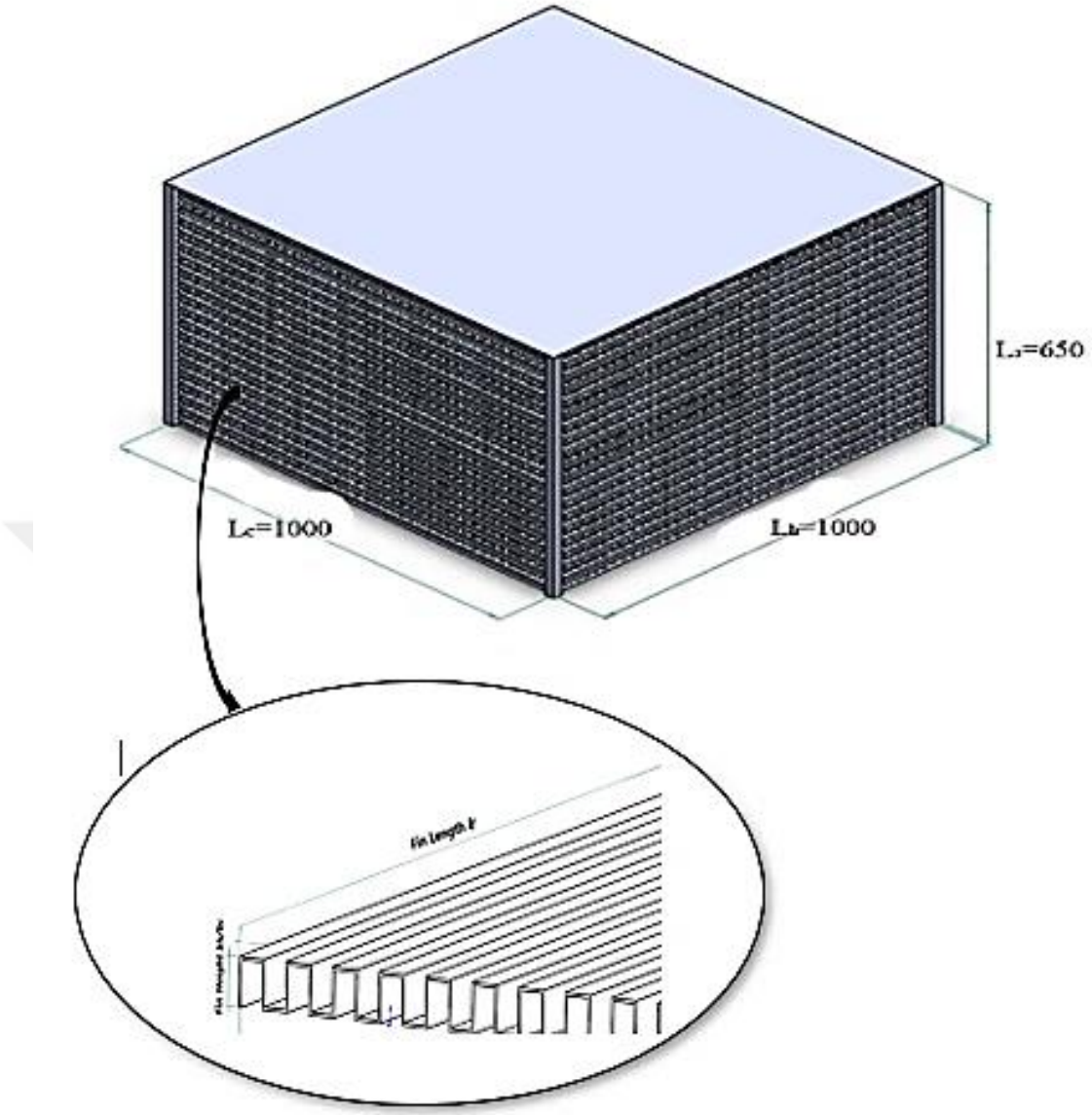

Figure 3.8. Heat Exchanger with main dimensions

CHAPTER 4 . RESULTS AND DISCUSSIONS

4.1. Design Results

After the design calculations were completed and a suitable value for the pressure drop was reached, the following results were obtained.

4.1.1. Input Data

1. Required Effectiveness: $\varepsilon = 0.8381$
2. Fin height: $b_h = b_c = 15mm$
3. Fin thickness: $\delta_w = 1mm$, $\delta_h = \delta_c = \delta_w$
4. Heat transfer surface area density: $\beta_c = \beta_h = 2000m^2/m^3$
5. Fin area/total area ratio: $\left(\frac{A_f}{A}\right)_h = \left(\frac{A_f}{A}\right)_c = 0.785$
6. Hydraulic diameter: $D_{h,h} = D_{h,c} = 1.6mm$
7. Fluid mass flow rates: $\dot{m}_h = 1.66kg/s$, $\dot{m}_c = 2.0kg/s$
8. Pressure drop : $\Delta P_h = 9.0kPa$, $\Delta P_c = 8.79kPa$
9. Plate Thermal heat transfer (Both plates are made of steel): $k_w = 33W/mK$
10. Inlet Temperatures of gases: $T_{h,i} = 798K,\ T_{c,i} = 317K$

4.2. Thermodynamic properties of Heat Exchanger

Table 4.1. Fluid properties.

	$\mu(10^3)$	c_p(kJ/kgK)	P_r	$P_r^{2/3}$
Hot air stream ($T_{h,m}$)	305.8	1.051	0.685	0.777
Cold air stream ($T_{c,m}$)	270.1	1.030	0.684	0.776

Table 4.2. Fluid Densities.

	$T_i(K)$	$T_o(K)$	$\rho_i(kg/m^3)$	$\rho_o(kg/m^3)$	$\rho_m(kg/m^3)$
Hot air stream	798	394.87	0.4354	0.8711	0.5804
Cold air stream	317	658.42	1.1614	0.5356	0.6964

Table 4.3. Fluid Flow Properties.

	Re	***j***	***f***	***ntu***	$h_i(W/m^2K)$	$G_i(kg/m^2s)$
Hot air stream	329.84	0.00 358	0.01963	10.790	30.53	6.3047
Cold air stream	415.57	0.00285 6	0.01477 7	9.139	26.59	7.0153

Table 4.4. Heat Exchanger Properties.

Coefficient/Property	**Value**	
	Cold Air Stream	**Hot Gas Stream**
Outlet Temperature $T_{i,o}$	685.42 K	394.87 K
NTU	5.395	
Core Velocity G_i	7.0153 kg/m^{2}s	6.3047 kg/m^{2}s
Reynolds Number Re_i	415.57	329.84
j-factor j_i	0.02856	0.0358
f-factor f_i	0.014777	0.01963
Heat transfer Coefficient h_i	305.3 W/m^{2}K	265.9 W/m^{2}K
Fin Efficiency $\eta_{f,i}$	0.9779	0.9747
Overall Surface Efficiency η_o	0.983	0.980
Overall Heat Transfer Coefficient U	139.5 W/m^{2}K	
Maximum Heat transfer between Fluids Q_{max}	3795.2 kW	
Heat transfer between Fluids Q	3180.8 kW	

Table 4.5. Heat Exchanger Dimensions.

Feature	**Calculated Value**		**Rounded Value**
	Cold Air Stream	**Hot Air Stream**	
Total Surface Area A (m^2)	674.86	674.86	-
Minimum free flow area A_o (m^2)	0.2851	0.2635	-
Frontal Area A_{fr} (m^2)	0.6740	0.6229	-
Air Flow Length (m)			
Lc	0.947	-	1.0
Lh	-	1.024	1.0
L_3 (Height)	0.648		0.650

The final design of our heat exchanger is of the compact plain plate fin type with crossflow fin arrangement. Each side is made up of sheets with plain rectangular fins (Figure 4.1). The superposing fins are separated from each other by thin metal sheets (Figure 4.2) and these metal sheets are supported on the four corners by supporting

bars (Figure 4.3). On the four sides of the heat exchanger are found side covers (Figure 4.4) on which we have the air and gas inlets and outlets. Below are detailed presentations of the different parts of the heat exchanger. The full design drawings and specifications of the different parts of the heat exchanger are also presented in the appendix section.

1. Fins

Fin property	Optimised value (mm)
Length	500
Height	15
Thickness	1

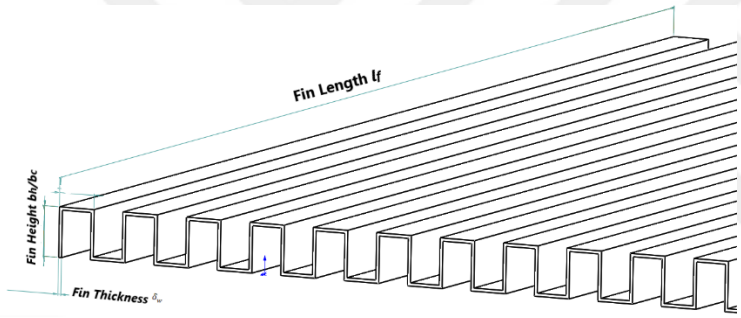

Figure 4.1. Heat exchanger Fin Dimension

2. Separating plate

The separating plate is made of stainless steel with a 1 mm thickness. See figure below

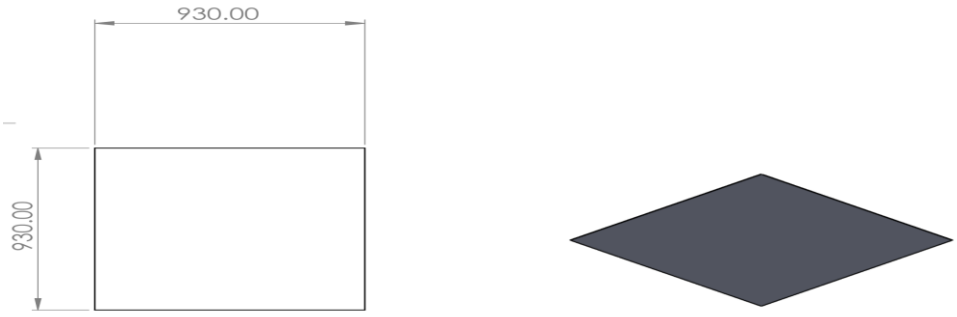

Figure 4.2. Separating plate

3. Supporting bar

The supporting bars are made of rectangular steel rods. Below are their specifications

Table 4.6. Supporting Bar Dimensions

Property	Final value (mm)
Length	500
Width	20
Thickness	20

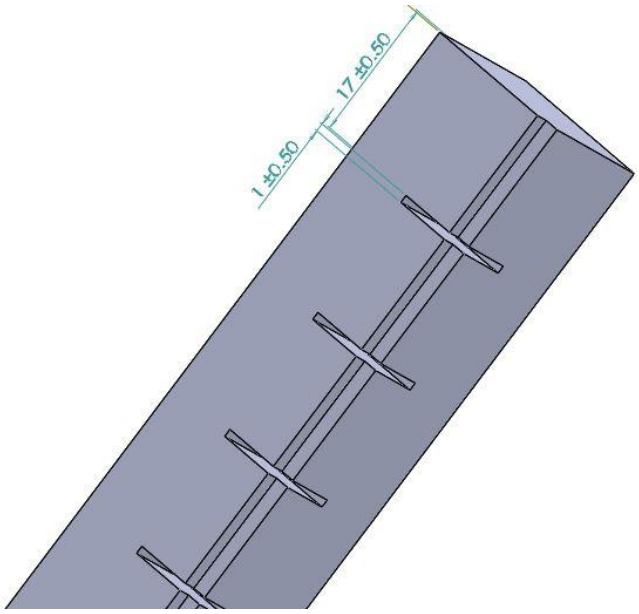

Figure 4.3. Supporting bar

4. Side cover

The side covers are made of steel and are used to cover the 4 sides of the heat exchanger. Each side cover has two tube inlet support for the inlet and outlet of the fluids.

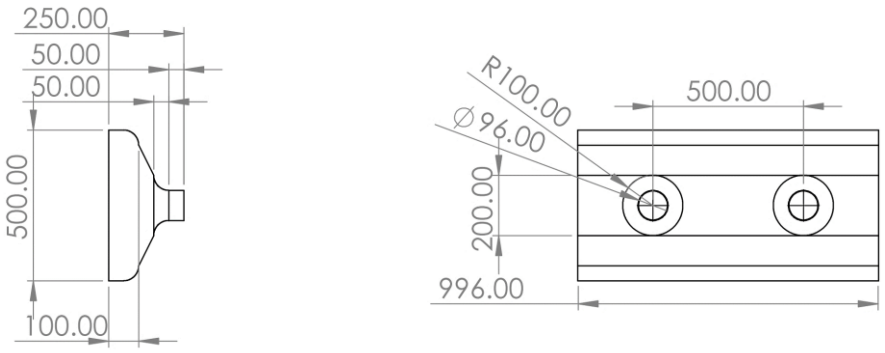

Figure 4.4. Side cover

5. Heat exchanger

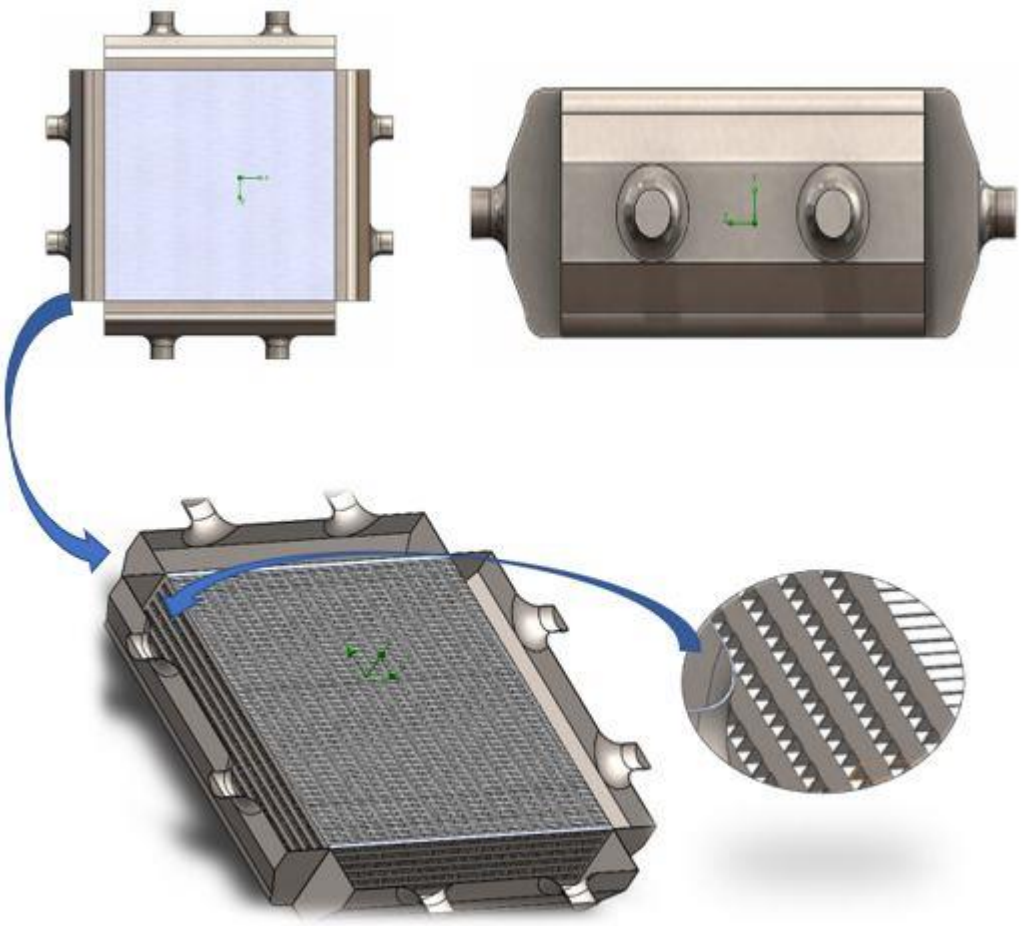

Figure 4.5. 3D Heat exchanger model

4.3. Heat exchanger CFD Simulation.

After the final design of the heat exchanger was drawn using an appropriate CAD tool, the obtained model was now ready for simulation testing. The CFD simulation was performed using Solidworks Flow Simulation.

4.3.1. Simulation Setup.

a. Mesh settings

During our simulation we applied Finite Volume Method (FVM) solving approach. In this approach, the size and shape of the 3D model and fluid space remains constant but the mesh itself can change and update during the simulation. The FVM allows a solution-adaptive meshing, where the solver can refine and improve the meshing during the calculations without starting from scratch.

During the first mesh setup we applied a Global Mesh with the following meshing configuration. The total number of mesh cells was at 17126282 and the number of fluid cells was 11623742, solid cells 5502540 and the number of fluid cells containing sold was 5356559.

Mesh Structure	Mesh size	Breakdown level
Rectangular	0.01 m	2

Mesh optimisation

After the first run we optimised the meshing by applying a solution adaptive meshing with a tabular refinement and a level 2 refinement. The Approximate Maximum number of cells was set at 10 000 000. The maximum number of cells was set at this number so as to concentrate the meshing on important areas of the heat exchanger volume. After 254 iterations we attained convergence. The mesh before and after

optimisation is presented in Figure 4.6. From Figure 4.6b, the refinement level within the heat exchanger can be observed. The refinement level ranges from 2 within the fluid space (between the covers and the HE block) to 5 within the heat exchanger block. Thus, within the fins of the heat exchanger, each square cell of 0.01 m was broken down into 5 levels. As a result, providing a highly optimised mesh structure.

b. Boundary conditions

The boundary conditions for the CFD study were set as presented in Table 4.6. below. The study was done with the heat exchanger considered as an open system and the hot gas rejected into the atmosphere at atmospheric pressure.

Table 4.6. CFD Analysis Boundary Conditions

Hot stream inlet temperature	**Cold stream inlet temperature**	**Hot stream mass flow**	**Cold stream mass flow**	**Wall initial temperature**
798K	317 K	1.66 kg/s	2kg/s	293K

4.3.2. Governing equations

The underlying equations of this CFD problem are the solutions of the heat and mass flow equations of our heat exchanger. These equations are steady-state equations as expressed in chapter 3, equations 3.1-3.34. We also made use of transport equations for turbulence and viscosity equations 3.10 and 3.11.

4.3.3. Simulation results

The boundary conditions for the CFD analysis were as specified above in input data. The CFD analyses were carried within the boundary conditions as specified above. An

adaptive and automatic meshing structure was used in the simulation. The Figure 4.5. shows the meshed structure. In the final optimised structure (Figure 4.5. right), we used a minimum length and a solution adaptive mesh structure with a level 2 tabular refinement. This was appropriate for the simulation of our heat exchanger since it permits for an increased computational and storage savings, it accommodates the complexity of our structure and it is proper for our physical system since it makes the simulation independent of the heat exchanger size.

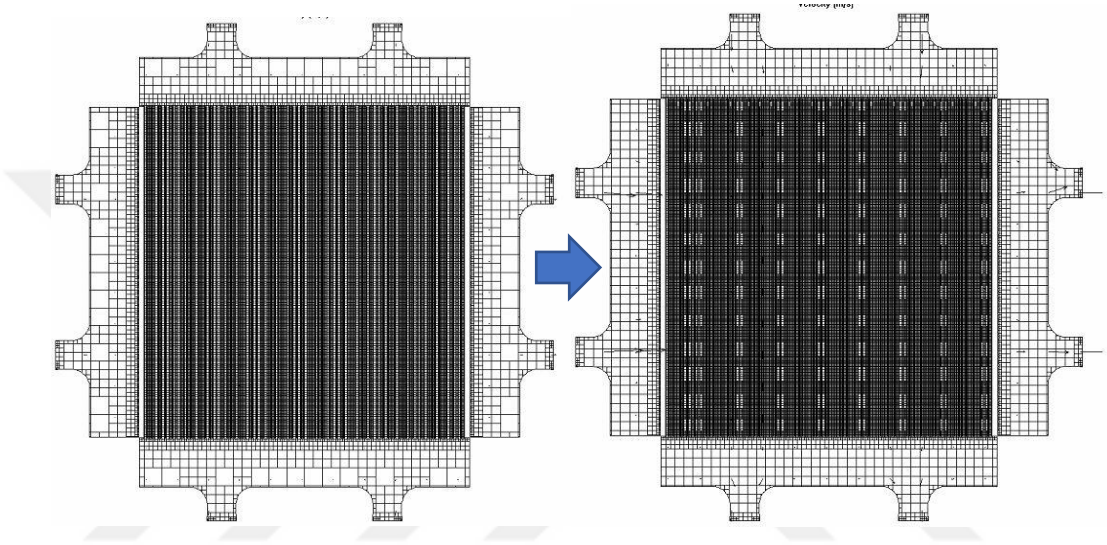

(a)

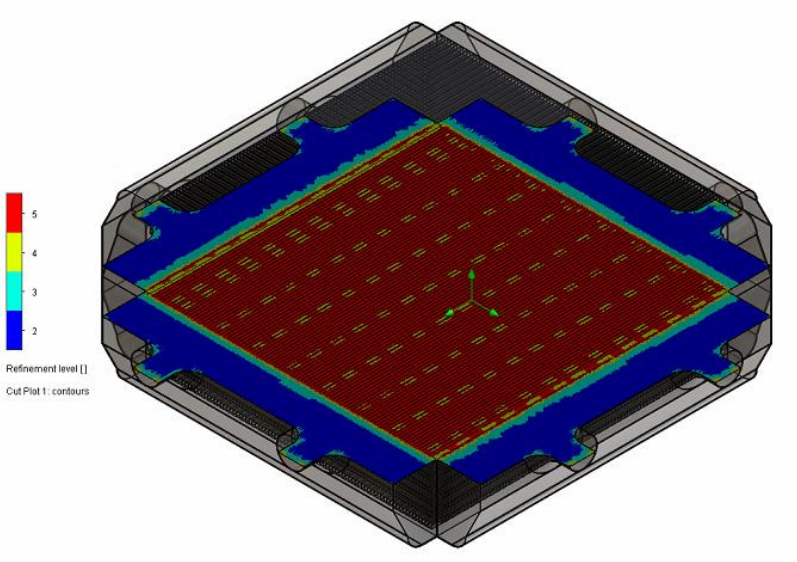

(b)

Figure 4.6. (a) Meshed Heat exchanger before and after refinement. (b) Mesh refinement level

During the simulations we applied a finite volume method (FVM) for simulation algorithm as described above. The results of the CFD study were as follows.

a) Temperature variation of cold air stream and hot gas stream outlet

The simulation was run at constant inlet air and gas temperatures and constant flows rates. The inlet temperatures of the fluid were set at 317 K and 798 K for the cold air inlet and hot gas inlet respectively. The initial solid or wall temperature of the heat exchanger was 294 K. The outlet temperature of the cold air stream outlet was then measured. The following graph was recorded. From Figures 4.7. and 4.8., we can observe that the heat exchanger heats up with time and then finally attains a constant outlet temperature on each of the streams. There is also a sharp drop in temperature after about 10000 seconds. Since the solid was at a lower temperature than the fluid, so during this period, the solid absorbs the heat from the fluid thus reducing its temperature. We also observe a convergence on all the outlets after 254 iterations. At convergence, the heat exchanger attained 560 K and 694 K on the air outlet and gas outlet ports respectively.

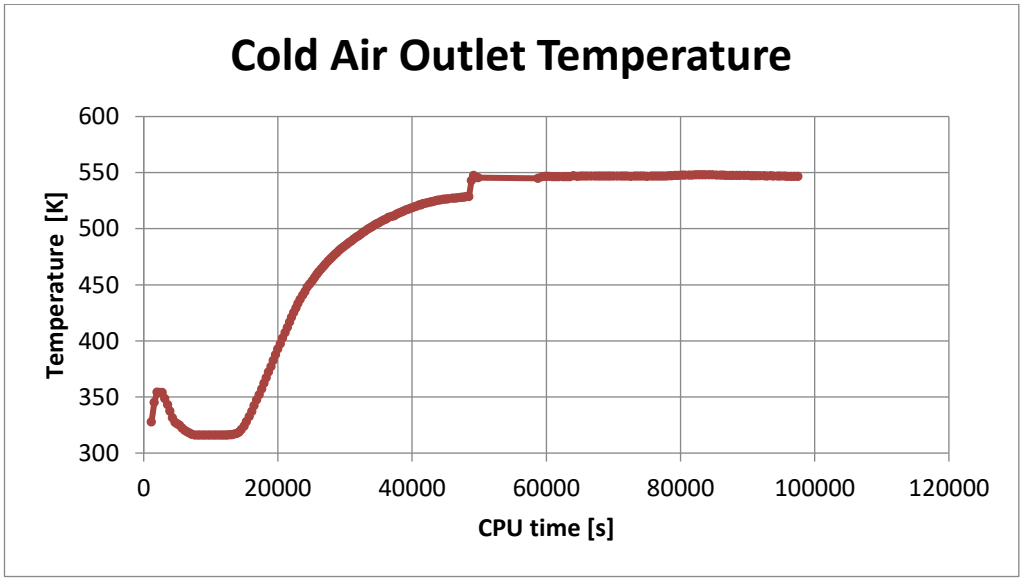

Figure 4.7. Simulations results of the cold air stream outlet temperature

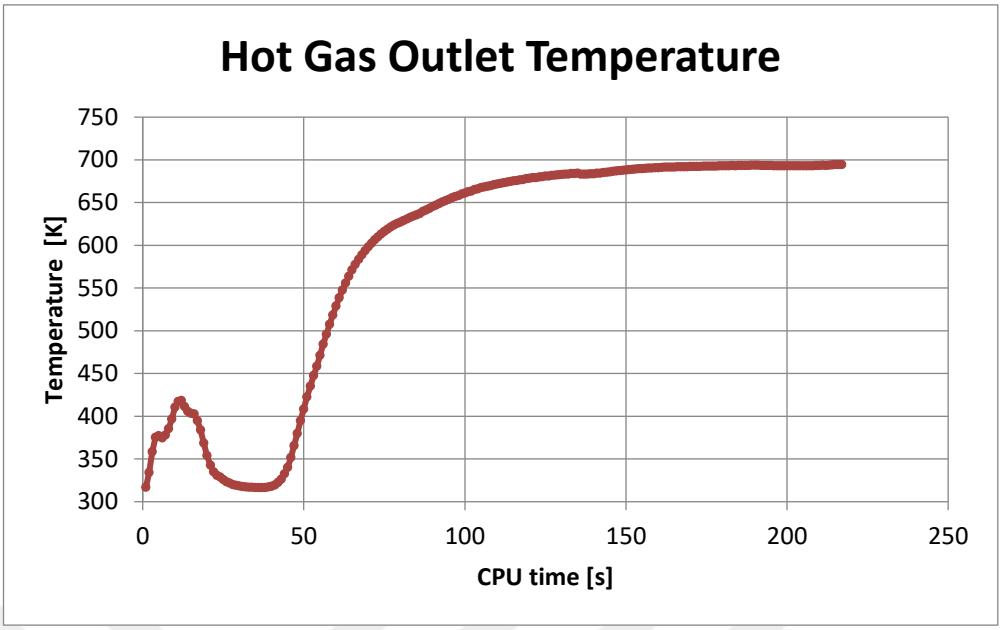

Figure 4.8. Simulations results of the hot gas stream outlet temperature

b) Fluid distribution in heat exchanger

After the CFD study was complete, a visualisation study was carried out so as to observe the fluid distribution within the heat exchanger. The Figure 4.8 was obtained. From the figure, it can be observed that the flow is well distributed within the exchanger with very little turbulence. There is also a bit of swirling effect observed between the heat exchanger cover and the heat exchanger block on the fluid entry sides.

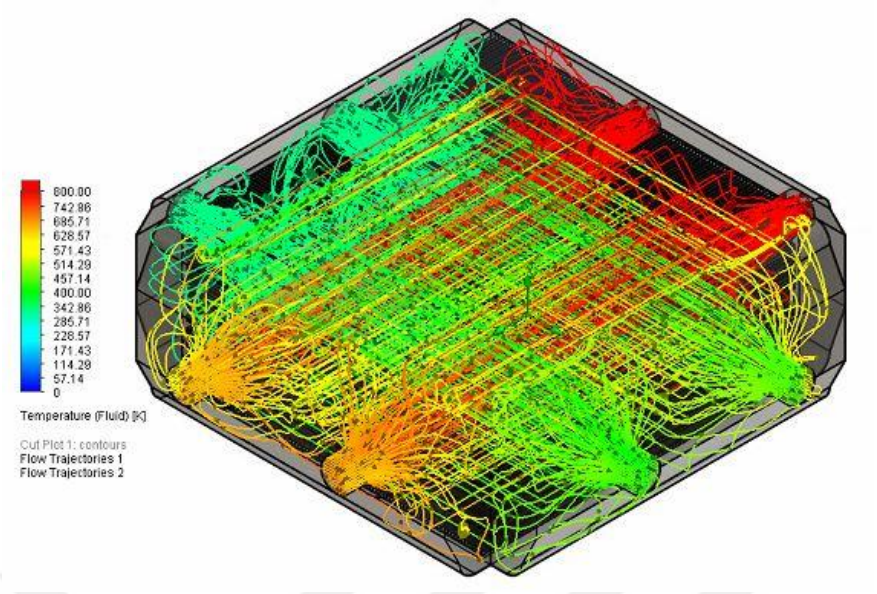

Figure 4.9. Flow trajectory within heat exchanger.

From Figure 4.9, we observe that the fluid is densest towards the cold air inlet. This is so because the fluid at that end is colder, so the air particles are heavier. Thus, making the fluid denser. The fluid density ranges from 0.46 kg/m^3 at the hot gas inlet end to 1.29 kg/m^3 at the cold air inlet end.

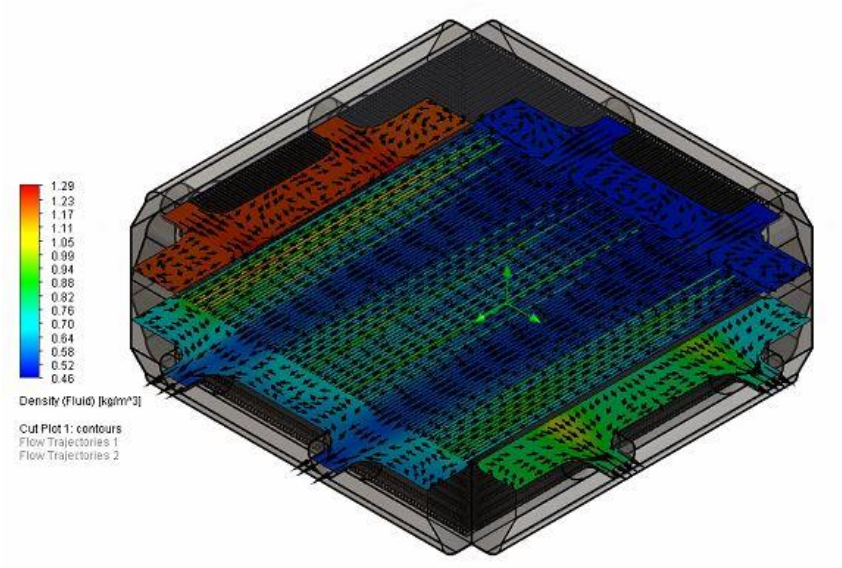

Figure 4.10. Fluid density distribution.

c) Heat distribution profile within the heat exchanger

During the simulation, the heat distribution profile of the heat exchanger was recorded. Figure 4.10 below shows the temperature variation within the heat exchanger. From the figure we can observe that the flow is well distributed inside the heat exchanger with the heat densely concentrated along the axis of the fluid entry ports. It can be observed that hot gas gradually losses its heat while transferring it to the cold air. Within the heat exchanger a minimum temperature of 315.568 K (at the air inlet) is recorded and a maximum temperature of 903.334 K (at the gas inlet). Along the cold air stream, we recorded a minimum temperature of 315.568 K and a maximum temperature of 560 K. It can also be observed that much of the heat transfer is done at the centre of the heat exchanger especially along the axes of the fluid entrance ports. Also, heat transfer is higher towards the hot gas entry end.

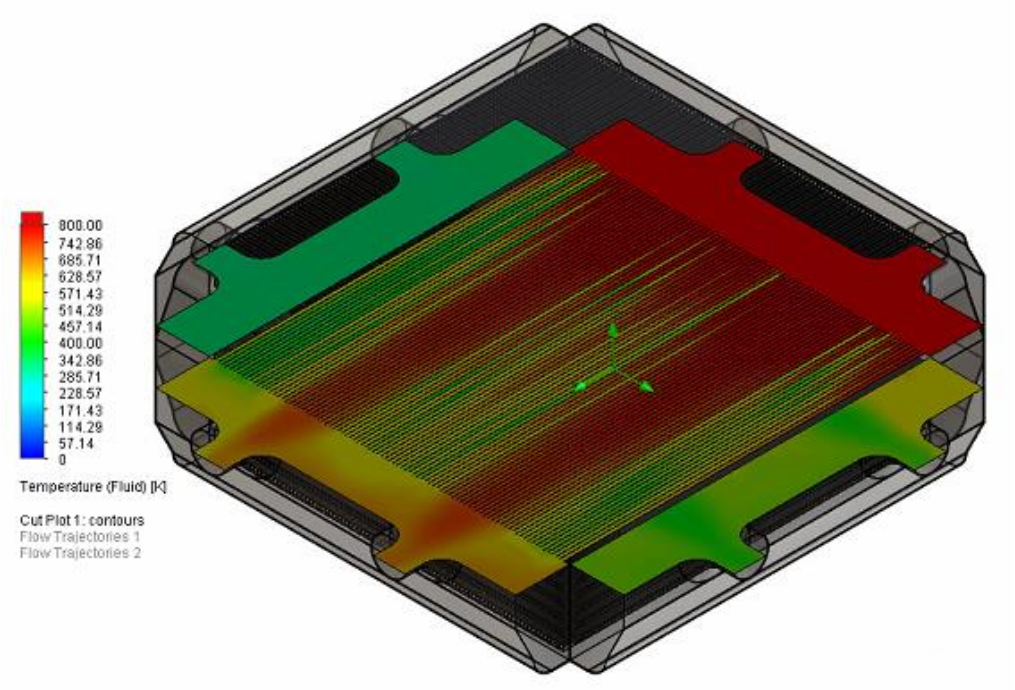

(a)

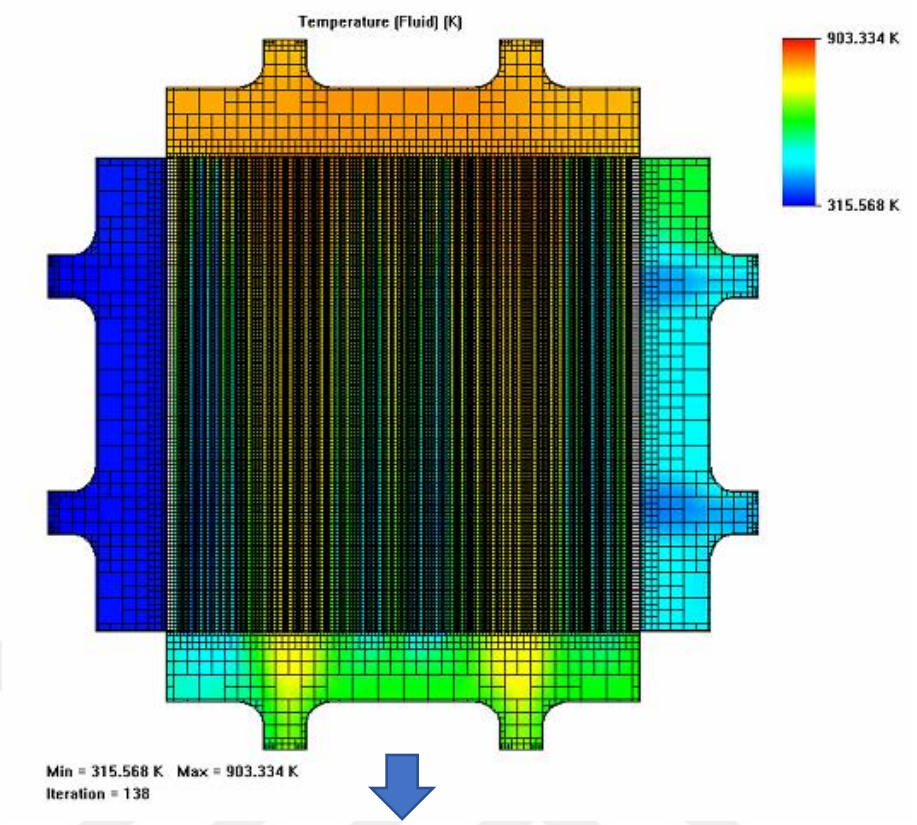
Temperature (Fluid) (K)
903.334 K
315.568 K
Min = 315.568 K Max = 903.334 K
Iteration = 138

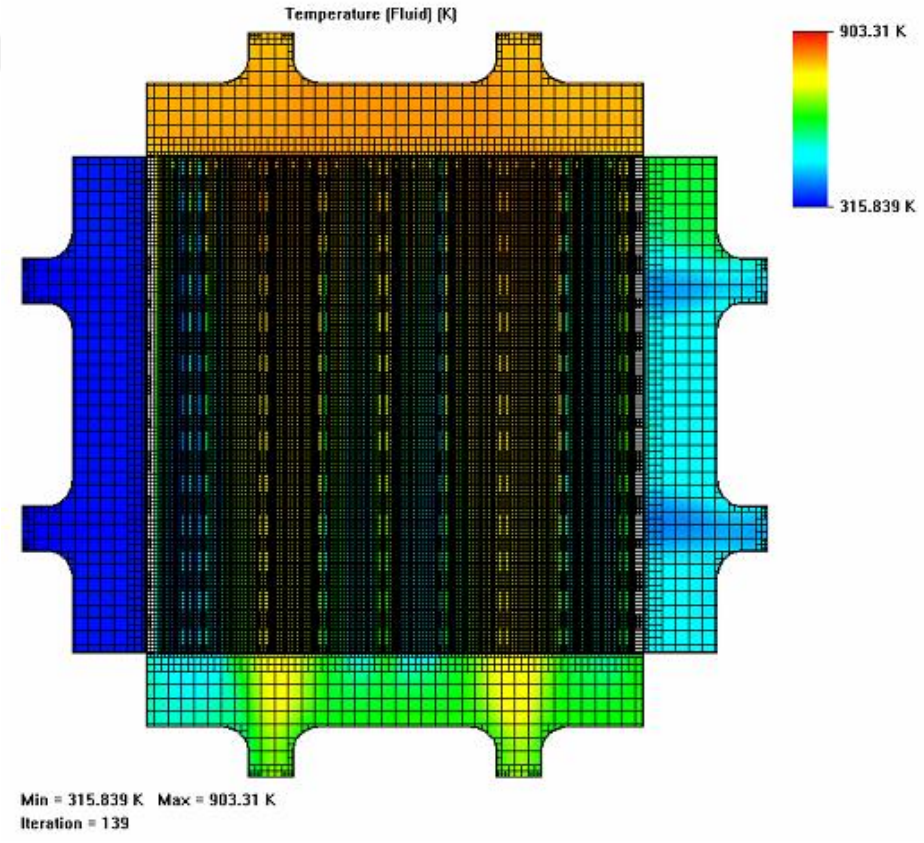
Temperature (Fluid) (K)
903.31 K
315.839 K
Min = 315.839 K Max = 903.31 K
Iteration = 139

(b)

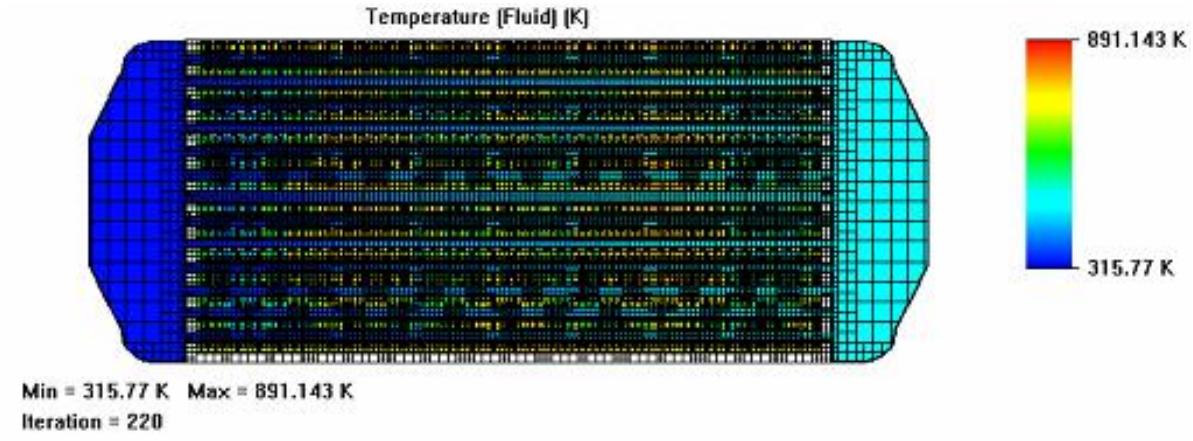

(c)

Figure 4.11. (a) 3D view of temperature distribution in HE (b) Top view of temperature distribution in HE before and after optimisation (c) Side View

After 254 iterations, the HE attained a convergence point and reached maximum operating state. Figure 4.12 shows the different outlet temperatures at convergence.

The fluid flow characteristics within the heat exchanger are summarised in table below.

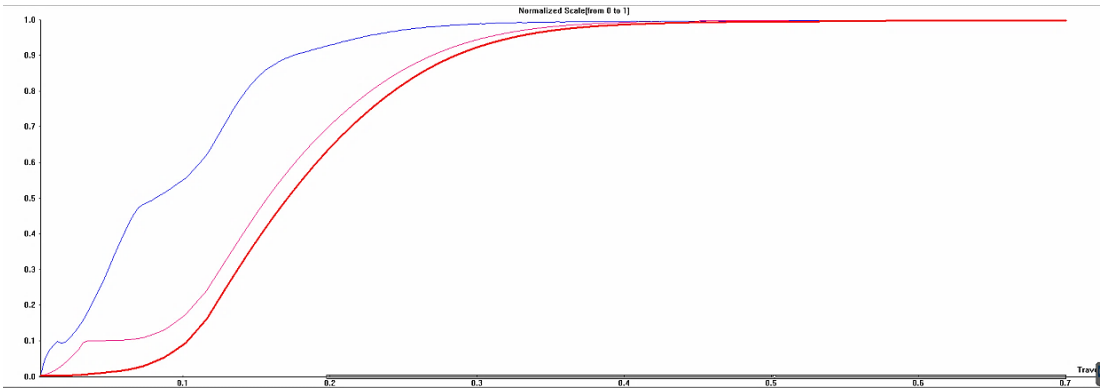

Figure 4.12. Temperature convergence plot.

Table 4.7. Fluid Flow Characteristics from CFD Simulation

Flow stream	Temperature (K)		Heat Transfer Coefficient (W/m^2K)	Heat Transfer Rate (kW)	Flow Velocity(m/s)
	Inlet	Outlet			
Cold Air	315.568	560	377	102.7	199.31
Hot Gas	903.334	694			148.84

d) Pressure Distribution within the Heat Exchanger

The pressure distribution profile within the heat exchanger is visualised in Figure 4.13. below. It can be observed that pressure within the heat exchanger is almost evenly distributed except along the line of contact of the cold inlet air and the heat exchanger block. This point is the highest pressure point within the heat exchanger. The pressure with the exchanger varies from 99213.92 Pa at the exit ports to 124638.28 Pa at the point of contact of the cold air stream with the heat exchanger block.

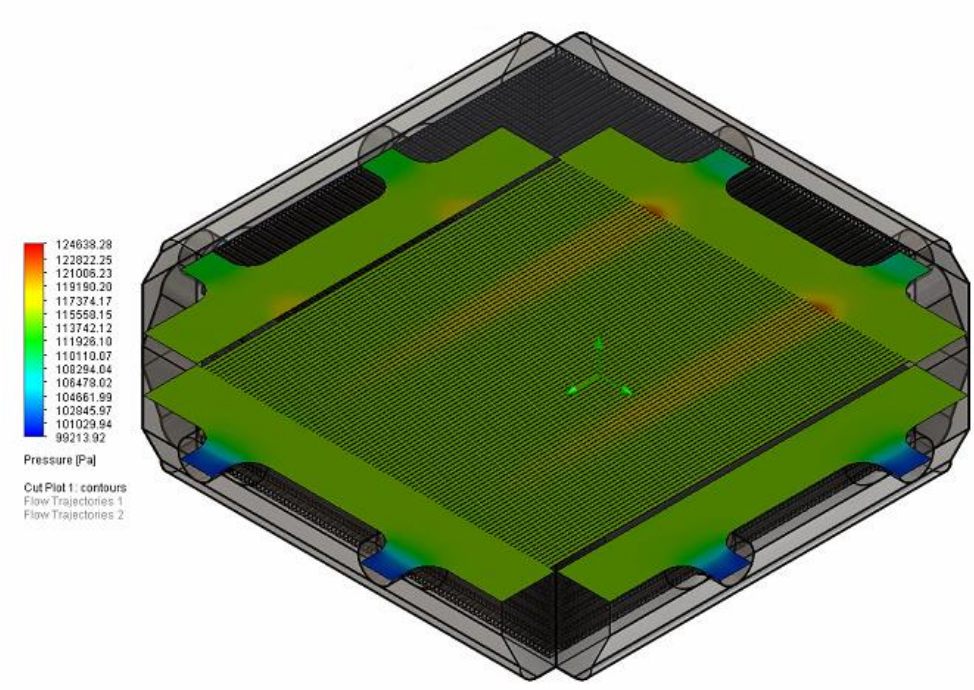

Figure 4.13. Pressure profile within heat exchanger.

4.4. Comparison of CFD Analysis Results with the Results of the Theoretical Analysis

After the CFD analysis was completed, the results of the fluid flow characteristics were obtained. Some of these results are presented in Table 4.7. above.

Table 4.8. Comparison of CFD and Theoretical analysis results

Property	Value			
	Theoretical Analysis		CFD Analysis	
	Cold stream	Hot stream	Cold stream	Hot stream
Inlet Temperature	317 K	798 K	315.658 K	903.334 K
Outlet Temperature	685.4 K	394.9 K	560 K	693 K
Heat Transfer Coefficient	139.5 $W/m^2 K$		377 $W/m^2 K$	
Heat Transfer Rate	3795.2 kW		102.7 kW	
Wall Temperature	538.42 K		560 K	

From the results table above, we can observe that there are variations in the results between the two analysis. These variations are can are as a result of the following; during the theoretical analysis, the heat exchanger is considered as a close system with ideal conditions. Thus, there is perfect transfer of heat from one medium to another. Also, during the theoretical study, the mass flow rate is not considered when determining the outlet temperature of the hot gas outlet. Whereas the hot gas mass flow rate has an influence on the outlet temperature of the gases and thus their transfer rate. However, for the CFD study, the system is considered as an open system with hot gas being released at atmospheric temperature. Furthermore, during the CFD study, the heat exchanger body is first heated in order to bring it up to the fluid temperature.

Whereas in the theoretical analysis, the heat exchanger body and the fluid are considered to be at the same initial temperature.

Also, in the theoretical study, a heat transfer rate of 3795.2 kW was calculated whereas during the CFD analysis we recorded a heat transfer rate of 102.7 kW. This variation in values can be attributed to the fact that during the theoretical analysis, the gas mass flow rate was not considered in the determination of the outlet temperature of the hot stream which is a determining factor for the calculation of the heat transfer rate.

4.5. Parametric Analysis of the Heat Exchanger

4.5.1. Effects of fin length

The Figure 4.14. presents the relation between the heat exchanger fin efficiency versus the fin length at different values of fin height. It can be seen that the fin length has no effect on the fin efficiency. But as the fin height increases, there is a decrease in the Fin Efficiency. As shown by Figure 4.14., fin length does not have any effect on the Overall Surface Efficiency of the heat exchanger and with Fin Efficiency, the increase in fin height has a negative effect on the Overall Surface Efficiency. PFHE with taller fins are less efficient than those with shorter fins. This is so because the taller the fins, the smaller the ratio between the fin-fluid contact surface area and the volume of fluid. As a result, the less efficient the fins become.

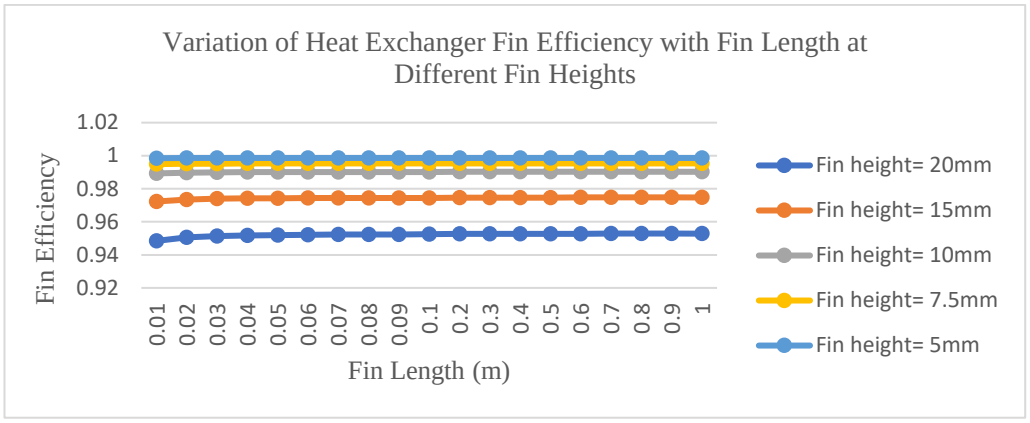

(a) Fin Efficiency

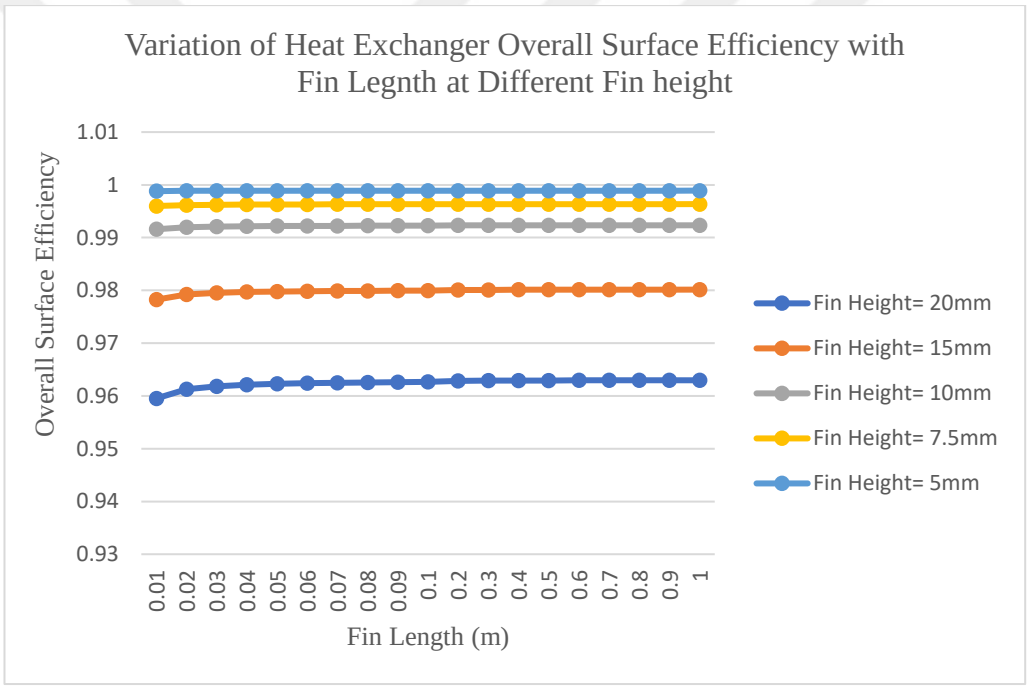

(b) Overall Surface Efficiency

Figure 4.14. Variation of Heat Exchanger Fin Efficiency and Overall Surface Efficiency versus Fin Length at different values of fin height.

4.5.2. Effects of fin thickness

As presented in Figure 4.15., the relationship between the heat exchanger fin efficiency and overall surface efficiency versus the fin thickness can be seen. The Figure 4.15.

also shows the effects of the fin height on these relations. As we can see on Figure 4.15a and Figure 4.15b, the fin thickness has a significant effect on the fin efficiency and the overall surface efficiency. As the fin thickness increases, the fin efficiency and overall surface efficiency decrease as well. This is so because the thicker the fins, the more time it takes for the heat to be transmitted across the fin. Thus, reducing its efficiency. Also, as the fin height increases, there is a shift in the fin efficiencies with a slight increase in the fin efficiencies. Increasing the fin height increases the heat transfer area thus increasing the efficiency of the fins. Also, increasing the fin height widens the fluid flow passage and thus increasing the fluid flow rate. Similar observations were made by Javaherdeh et al 2018, [39].

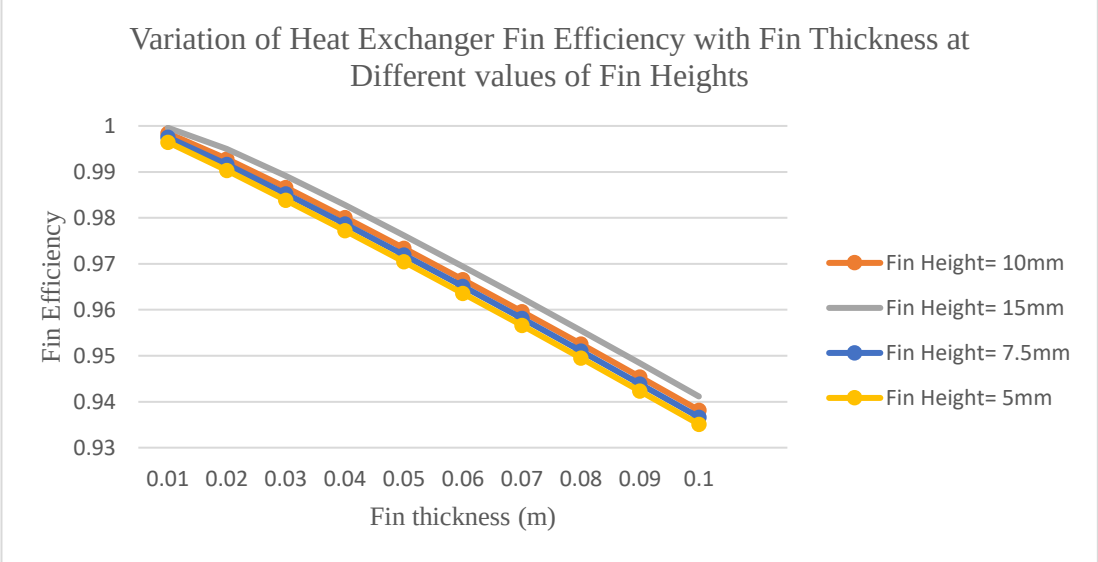

(a) Fin efficiency

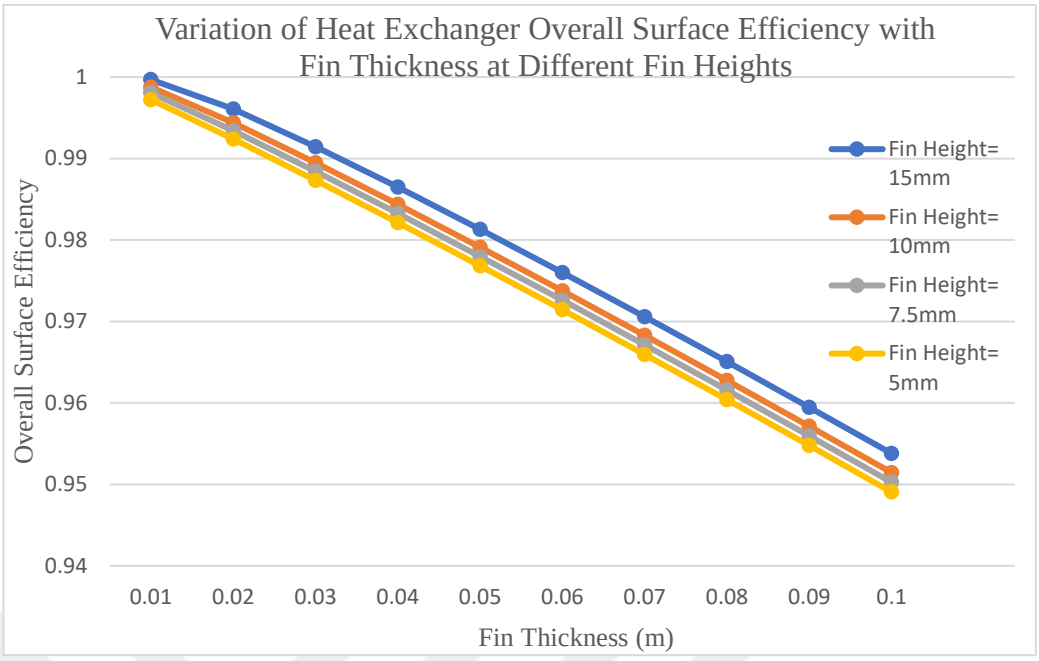

(b) Overall surface Efficiency

Figure 4.15. Variation of Heat Exchanger Fin Efficiency and Overall surface Efficiency with Fin Thickness at different fin heights (other parameters are constant as stated in the design specifications).

4.5.3. Effects of hot gas stream mass flow rate

The Figure 4.16. presents the relationship between the hot gas stream mass flow rate and the cold air stream outlet temperature (the air from the compressor). This relationship is examined at different values of the Effectiveness Value, the cold air stream inlet temperature, and the hot gas stream inlet temperature. It can be observed that the hot gas flow rate has a positive effect on the cold air stream outlet temperature. The graphs show an increasing linear relationship between the two variables. From Figure 4.16a and 4.16b, an increase in effectiveness value positively affects the cold air stream outlet temperature same as observed by Thakre et al 2016 [40]. Also, at lower mass flow rates, the deviation in outlet temperature is insignificant. But as the mass flow rate increases, the deviation becomes more important.

The mass flow rate is the mass of fluid that flows through a unit volume per second. An increase in the hot gas mass flow rate signifies more hot gas particles flowing within the heat exchanger per second, therefore the greater the amount of heat transferred to the cold air. Nevertheless, these calculations are done with assumption that the PFHE is a closed system and without taking into consideration the length of travel of the fluid.

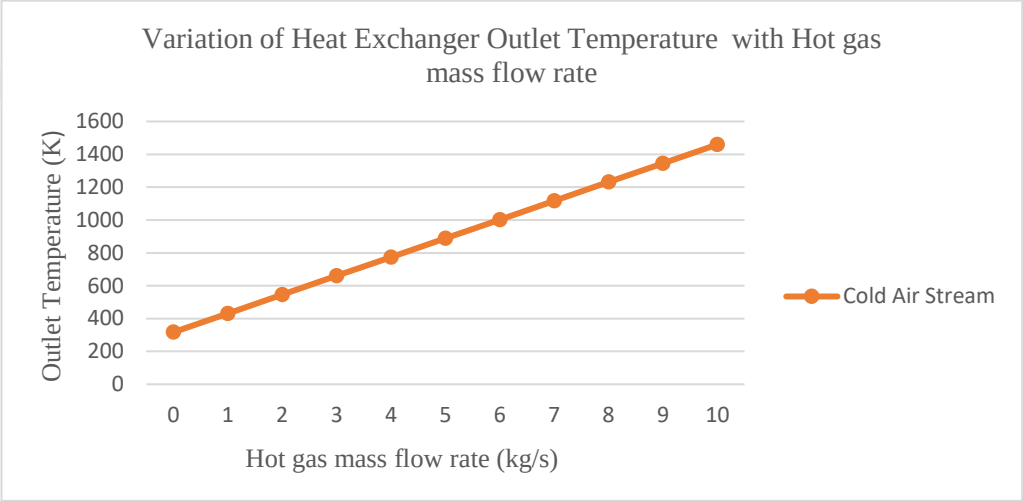

Figure 4.16. Cold air stream and hot gas stream outlet temperatures versus hot gas mass flow rate.

The increase in cold air stream inlet temperature has a converging effect on the cold air stream outlet temperature at lower mass flow rates (Figure 4.16c). This happens until it reaches the convergence point. From this point, as the cold air stream inlet temperature increases, the cold air outlet temperature decreases. This point of convergence is the when the cold air stream inlet temperatures equals the hot gas stream inlet temperatures. So, after this point, the direction of heat flow interchanges. Panthee had similar observations in his thesis, [41].

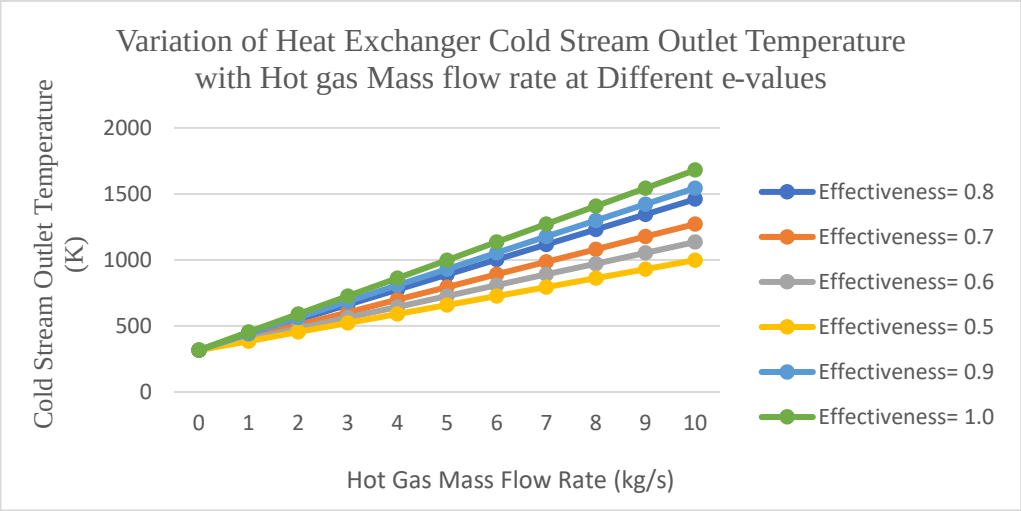

(a) Effectiveness value (e)

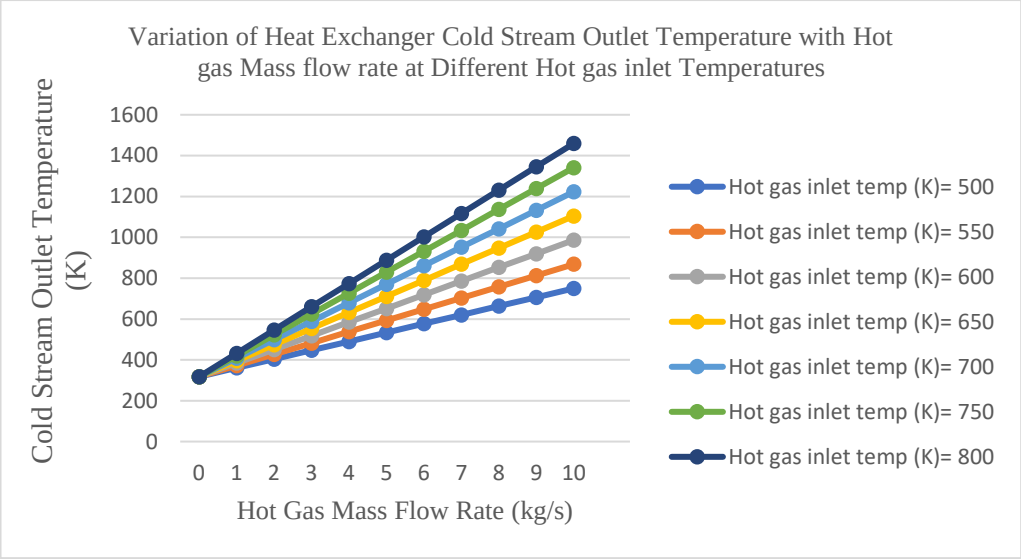

(b) Hot gas stream inlet temperature

The fin efficiency, overall surface efficiency and outlet temperatures of a PFCHE depends on the operating conditions (mass flow rates and inlet temperatures of fluids), and the heat exchanger design parameters (fin length, height, thickness and the effectiveness value). The variation of fin height at lower fin thickness is very significant for the heat exchanger fin efficiency as well as for the overall surface efficiency as shown by Figures 4.15a and 4.15b. The fin length has little effect on the fin efficiency and overall surface efficiency of the heat exchanger (Figure 4.17). The outlet temperatures of the heat exchanger are also very much affected by the effectiveness value. This influence is more important at higher gas mass flow rates

(Figure 4.17a). At higher gas mass flow rates, the hot gas inlet temperature has a crucial influence on the air outlet temperature (Figure 4.17b). The air inlet temperature has an inverse effect on the air outlet temperature above the convergence point (Figure 4.17c). This is due to the inverse in the direction of heat flow since above this point the air inlet temperature is greater than the gas inlet temperature. Also, the gas mass flow rate has no influence on the gas outlet temperature (Figure 4.16.).

Figure 4.16. presents the relation between the outlet temperatures of the two streams versus the gas mass flow. It is observed that the gas mass flow rate has no effect on the hot gas stream. But it has a positive effect on the cold air stream. This observations can also be seen the work done by [41–45]. From Figures 4.15. and 4.16., it can be seen that; using thinner and shorter fins will produce efficient and more compact plain fin compact heat exchangers. A 50% reduction in fin height can cause as much as an 18% increase in the fin efficiency of the heat exchanger. This can be considered when there is a problem of space. But this will also require advanced manufacturing techniques and thus incurring more cost.

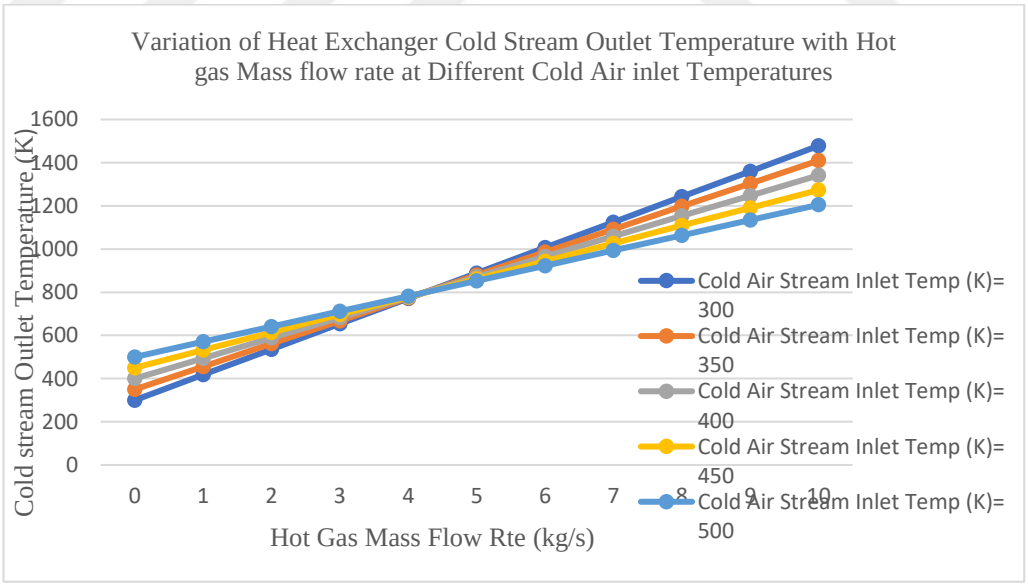

(c) Cold air stream inlet temperature

Figure 4.17. Variation of Heat Exchanger Outlet Temperatures with Hot gas Mass flow rate (other parameters are constant as stated in the design specifications).

From the Figures 4.17., it can be seen that plain fin compact heat exchangers with higher effectiveness values attain higher outlet temperatures. For example, a 50% increase in the effectiveness value can cause as much as a 40% increase in the outlet temperature. Furthermore, as the fluid flow rate increases, this effect of the e-value on the outlet temperature also increases (with values of 15% at 1 kg/s, 34% at 5 kg/s and 40.1% at 10 kg/s). Also, to obtain higher outlet temperatures on the cold stream, the hot gas flow rate (flow velocity) can be increased. These results were obtained based on ideal conditions but experimental works done by other researchers obtained similar results. For example in Panthee's work, for plate heat exchangers he registered a 20 % increase in e-value and a 9 % increase in outlet temperature for a 50% change in mass flow rate of hot gas [41].

CHAPTER 5. CONCLUSION AND RECOMMENDATIONS

In this work, the main objective was to design and analysis a heat exchanger for a small-scale gas turbine with the aim of increasing its overall efficiency. The work started with a preliminary study of heat exchangers, their features and their various areas of application. This study permitted us to define the appropriate heat exchanger for our study. This choice is done taking into consideration some other factors like space, working fluids, operating temperatures, etc. From this, the Plain-Fin Compact Heat Exchanger (PFCHE) with rectangular fins and a crossflow arrangement is then selected as the suitable heat exchanger type for our study. The second section of the work takes a deep look at the available literature on the heat exchanger technology. This review is started with a thorough look at the different works done on the development of gas turbines. This is followed by a look at heat exchangers and their applicability. The review is then ended with a deep look at the compact heat exchanger, its applicability and the advancements throughout the years. In the last part of this section, the application of heat exchangers in gas turbines is examined. The fundamental governing equations are discussed. Also, the effects of the heat exchanger on the overall efficiency of the gas turbine is examined.

In the third section, the problems statement is restated and the initial conditions and design specifications are also stated. The materials of the heat exchanger are also determined. After which the manufacturing processes and approaches are discussed. In the second part of this section, the mathematical model of the different aspects of the heat exchanger are developed. This is done following the algorithm proposed by shah [33]. After the adaptation and refinement of the derived model, the final design model of the heat exchanger is obtained. This model is then developed with a suitable CAD tool to come out with a 3D design which is then run for simulation using suitable CFD tools. The results of the CFD study are obtained and analysed. The final design of the PFHE is made up of 38 fin plates (19 for the hot gas stream and 19 for the cold

air stream). Each fin plate has 84 fins giving a total of 3192 fins. Each fin has a length of 1 meter, a thickness of 1 mm and a height of 15 mm. The external dimensions for the heat exchanger are 1 m length, 1 m width and a height of 0.65 m. The full dimensions and properties of the design are presented in the Table 4.4. and Table 4.5.

These results can be summarised as follows The PFCHE is the suitable heat exchanger configuration for our study. The heat exchanger can raise the temperature of the inlet air into the combustion chamber of the gas turbine from 317 K to 678 K (in theory) and from 315 k to 560 K (during CFD simulation). Thus, increasing the efficiency of the gas turbine since the gas turbine is a function of the inlet temperature into the combustion chamber (T_3). The efficiency of the heat exchanger is affected by the fin length, thickness, and the effectiveness value of the heat exchanger. Furthermore, at higher mass flow rates, the effect of the effectiveness value on the efficiency of the heat exchanger is greater.

During this study, experimental or analytical studies could not be found on a similar heat exchanger with similar design and configuration. So, data could not be gotten for comparative analysis. Due to the shortcomings during this study, it is recommended that comparative study be carried out between experimental data and simulation results. This is to check if there are any disparities. Also, more parameters for analysis could be included in future studies. Furthermore, a rating study can be carried on the heat exchanger design so as to optimise its performance and its size.

REFERENCES

[1] Kakaç, Sadik; Liu, Hongtan; Pramuanjaroenkij A. HEAT EXCHANGERS 3rd Edition. CRC Press, Taylor & Francis Group; 2012.

[2] Thulukkanam K. Heat exchanger design handbook 2nd Edition. 2013.

[3] Cooper JK. CHARACTERISTICS, TYPES AND EMERGING APPLICATIONS. Nova Science Publishers, Inc. All; 2016.

[4] Focke WW, Knibbe PG. Flow visualization in parallel-plate ducts with corrugated walls. J Fluid Mech 1986;165:73–7. doi:10.1017/S0022112086003002.

[5] L. Wang, B. Sunden RMM. Plate Heat Exchangers_ Design, Applications and Performance. WIT Press; 2007.

[6] Sheik Ismail L, Velraj R, Ranganayakulu C. Studies on pumping power in terms of pressure drop and heat transfer characteristics of compact plate-fin heat exchangers-A review. Renew Sustain Energy Rev 2010;14:478–85. doi:10.1016/j.rser.2009.06.033.

[7] Morales AM. Compact heat exchangers and applications. n.d.

[8] Li Q, Flamant G, Yuan X, Neveu P, Luo L. Compact heat exchangers: A review and future applications for a new generation of high temperature solar receivers. Renew Sustain Energy Rev 2011;15:4855–75. doi:10.1016/J.RSER.2011.07.066.

[9] Hoerlle CA, Zimmer L, Pereira FM. Numerical study of CO2 effects on laminar non-premixed biogas flames employing a global kinetic mechanism and the Flamelet-Generated Manifold technique. Fuel 2017;203:671–85. doi:10.1016/j.fuel.2017.04.049.

[10] Hesselgreaves JE. COMPACT HEAT EXCHANGERS; Selection , Design and Operation. vol. 03. 1998.

[11] Shah RK. Advances in Science and Technology of Compact Heat Exchangers Advances in Science and Technology of Compact Heat Exchangers 2007;7632. doi:10.1080/01457630600559462.

[12] Lee H. Thermal Design_ Heat Sinks, Thermoelectrics, Heat Pipes, Compact Heat Exchangers, and Solar Cells (2010). Wiley; 2011.

[13] Southall D, Dewson SJ. Innovative Compact Heat Exchangers 2010:218–26.

[14] BAYRAK S. MODEL BİR TURBOJET MOTORUN, İKİNCİL YANMA İLE FARKLI YAKITLAR KULLANILARAK TEST EDİLMESİ. Sakarya University, 2018.

[15] Shah RK, London AL. Laminar Flow Forced Convection in Ducts. Laminar Flow Forced Convect Ducts 1978;94305:354–65. doi:10.1016/B978-0-12-020051-1.50020-6.

[16] Mcdonald CF, Massardo AF, Rodgers C, Stone A, Mcdonald CF, Rodgers C, et al. Recuperated gas turbine aeroengines . Part III : engine concepts for reduced emissions , lower fuel consumption , and noise abatement 2008. doi:10.1108/00022660810882773.

[17] Utriainen E, Sundén B. Numerical analysis of a primary surface trapezoidal cross wavy duct. Int J Numer Methods Heat Fluid Flow 2000;10:634–48. doi:10.1108/09615530010347213.

[18] McDonald CF. The increasing role of heat exchangers in gas turbine plants. Proc ASME Turbo Expo 1989;4. doi:10.1115/89-GT-103.

[19] Jeong JH, Kim LS, Lee JK, Ha MY, Kim KS, Ahn YC. Review of Heat Exchanger Studies for High-Efficiency Gas Turbines. ASME Conf Proc 2007;2007:833–40. doi:10.1115/GT2007-28071.

[20] Omar H, Kamel A, Alsanousi M. Performance of Regenerative Gas Turbine Power Plant 2017:136–46. doi:10.4236/epe.2017.92011.

[21] Picon-Nuñez M, Polley GT, Torres-Reyes E, Gallegos-Muñoz A. Surface selection and design of plate-fin heat exchangers. Appl Therm Eng 1999;19:917–31. doi:10.1016/S1359-4311(98)00098-2.

[22] Southall D, Pierres R Le, Dewson SJ. Design Considerations for Compact Heat Exchangers. Proc ICAPP 2008 2008:1953–68.

[23] Shah RK. Advances in Science and Technology of Compact Heat Exchangers Advances in Science and Technology of Compact Heat Exchangers 2007;7632:21. doi:10.1080/01457630600559462.

[24] Hwang SD, Jang IH, Cho HH. Experimental study on flow and local heat/mass transfer characteristics inside corrugated duct. Int J Heat Fluid Flow 2006;27:21–32. doi:10.1016/j.ijheatfluidflow.2005.07.001.

[25] Kanaris AG, Mouza AA, Paras S V. Flow and heat transfer in narrow channels with corrugated walls a CFD code application. Chem Eng Res Des 2005;83:460–8. doi:10.1205/cherd.04162.

[26] Gao W, Xu X, Liang X. Experimental study on the effect of orientation on flow boiling using R134a in a mini-channel evaporator. Appl Therm Eng 2017;121:963–73. doi:10.1016/j.applthermaleng.2017.04.019.

[27] Bobbili PR, Sunden B, Das SK. An experimental investigation of the port flow maldistribution in small and large plate package heat exchangers. Appl Therm Eng 2006;26:1919–26. doi:10.1016/j.applthermaleng.2006.01.015.

[28] Durmuş A, Benli H, Kurtbaş I, Gül H. Investigation of heat transfer and pressure drop in plate heat exchangers having different surface profiles. Int J Heat Mass Transf 2009;52:1451–7. doi:10.1016/j.ijheatmasstransfer.2008.07.052.

[29] Jeong JY, Hong H ki, Kim SK, Kang YT. Impact of plate design on the performance of welded type plate heat exchangers for sorption cycles. Int J Refrig 2009;32:705–11. doi:10.1016/j.ijrefrig.2009.01.028.

[30] Fernandes CS, Dias RP, Nóbrega JM, Maia JM. Laminar flow in chevron-type plate heat exchangers: CFD analysis of tortuosity, shape factor and friction factor. Chem Eng Process Process Intensif 2007;46:825–33. doi:10.1016/j.cep.2007.05.011.

[31] Spakovsky) ZS. Thermodynamics and Propulsion. n.d.

[32] D. Brian Spalding et al. HEAT EXCHANGER DESIGN HANDBOOK. 1983.

[33] Ramesh K. Shah, Dušan P. Sekulic. Fundamentals of Heat Exchanger Design. 2003.

[34] Pandey A. PERFORMANCE ANALYSIS OF A COMPACT HEAT EXCHANGER Department of Mechanical Engineering National Institute of Technology 2011.

[35] Southall D, Pierres R Le, Dewson SJ. Design Considerations for Compact Heat Exchangers 2008.

[36] Dewatwal J. DESIGN OF COMPACT PLATE FIN HEAT EXCHANGER. National Institute of Technology Rourkela, 2009.

[37] Shah RK, London AL. Laminar Flow Forced Convection in Ducts. Laminar Flow Forced Convect Ducts 1978;94305:354–65. doi:10.1016/B978-0-12-020051-1.50020-6.

[38] Aral MC, Hosoz M, Suhermanto M. Heat Transfer Modelling of a Parallel Flow Micro Channel / Louvered Fin Condenser Using Refrigerants R134a and R1234yf n.d.:1–11.

[39] Javaherdeh K, Vaisi A, Moosavi R. The effects of fin height , fin-tube contact thickness and louver length on the performance of a compact fin-and-tube heat exchanger 2018;36:825–34.

[40] Thakre PB, Pachghare PR. Performance Analysis on Compact Heat Exchanger. Mater Today Proc 2017;4:8447–53. doi:10.1016/j.matpr.2017.07.190.

[41] Panthee P. Testing and Characterising the Performance of Heat Exchangers 2017.

[42] P Moorthy, A N Oumer and MI. Experimental Investigation on Effect of Fin Shape on the Thermal-Hydraulic Performance of Compact Fin-and-Tube Heat Exchangers Experimental Investigation on Effect of Fin Shape on the Thermal-Hydraulic Performance of Compact Fin-and-Tube Heat Exchangers 2018. doi:10.1088/1757-899X/318/1/012070.

[43] Saari J. HEAT EXCHANGER DIMENSIONING. LAPPEENRANTA UNIVERSITY OF TECHNOLOGY, n.d.

[44] At, Xue Y, Ge Z, Du X, Hassan E. On the Heat Transfer Enhancement of Plate Fin 2018:1–18. doi:10.3390/en11061398.

[45] Doğan B. EXPERIMENTAL ANALYSIS OF THE EFFECT OF COLD FLUID INLET TEMPERATURE ON THE THERMAL PERFORMANCE OF A HEAT EXCHANGER 2016;2:583–92.

ANNEX

ANNEX I. Heat Exchanger Block

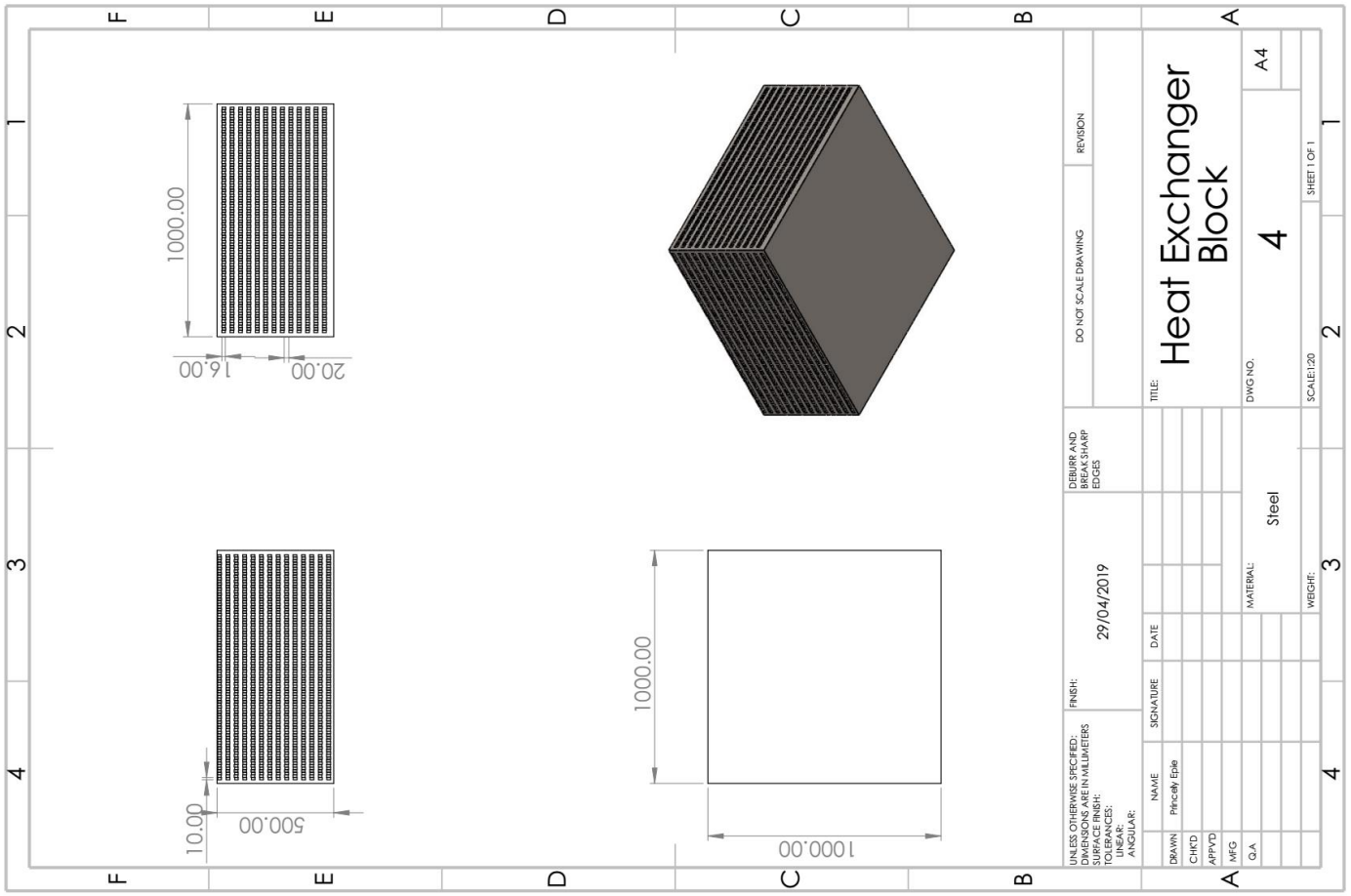

ANNEX II. Heat Exchanger

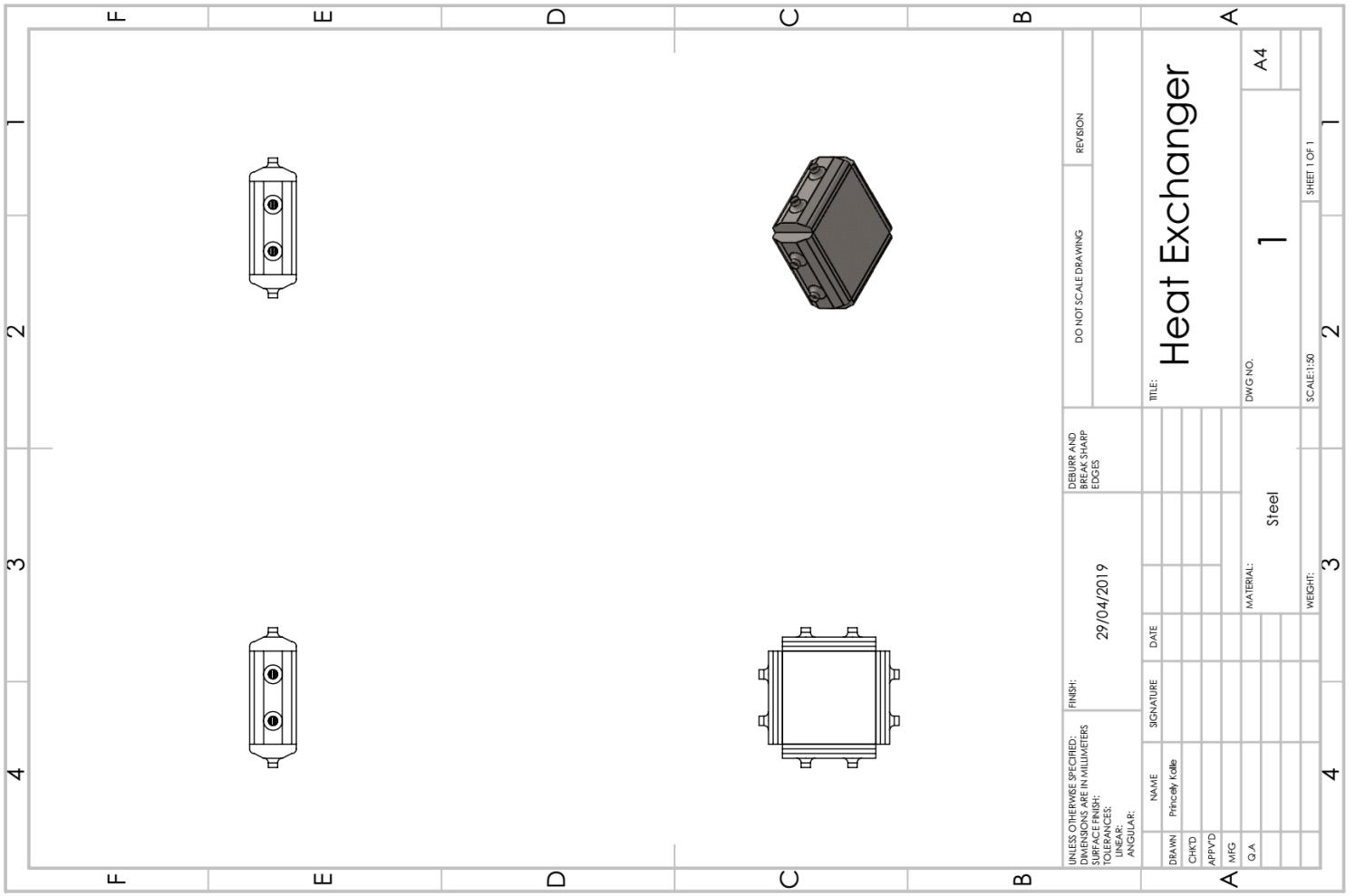

ANNEX III. Separating Plate

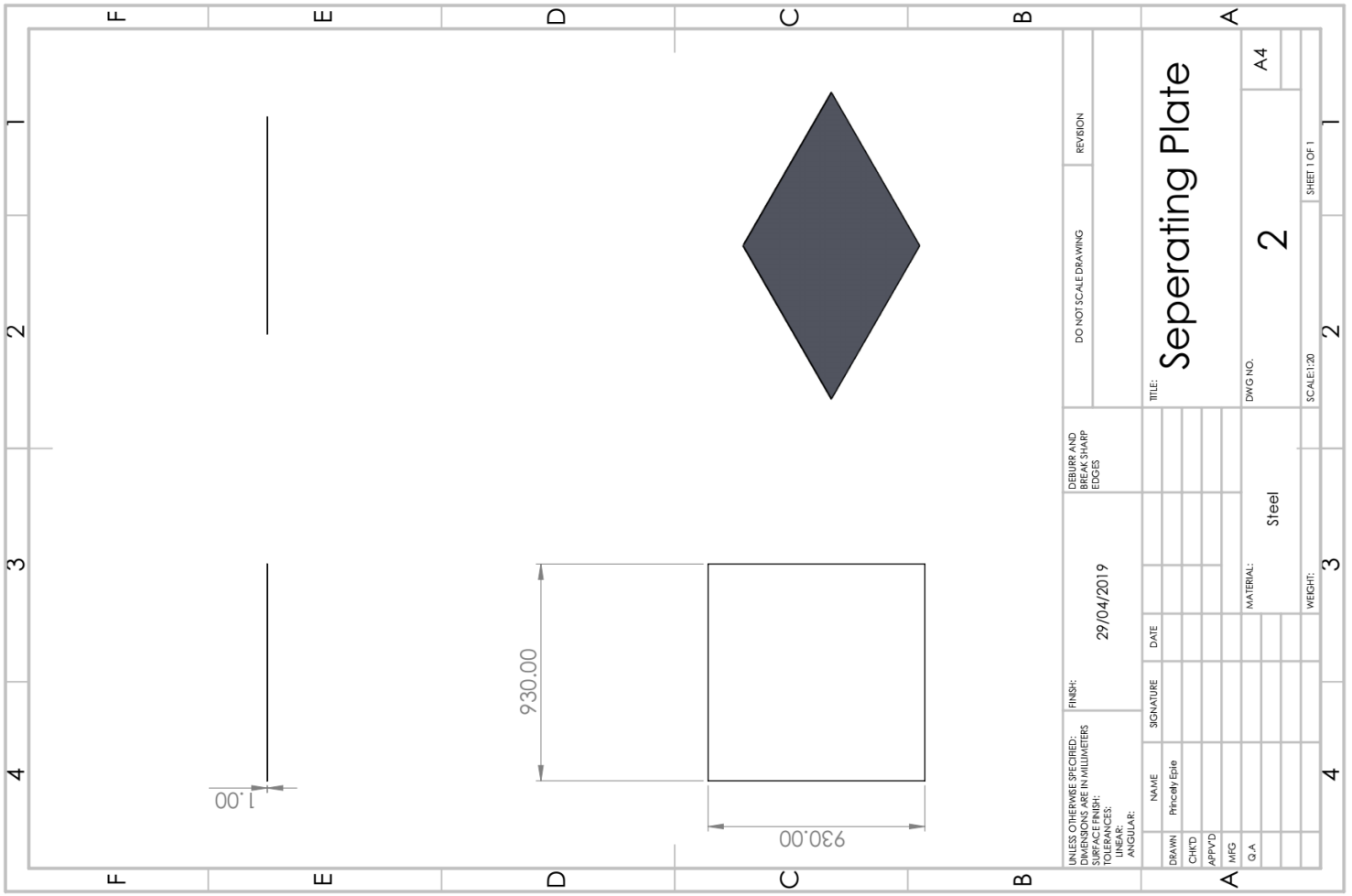

ANNEX IV. Heat Exchanger Side Covers

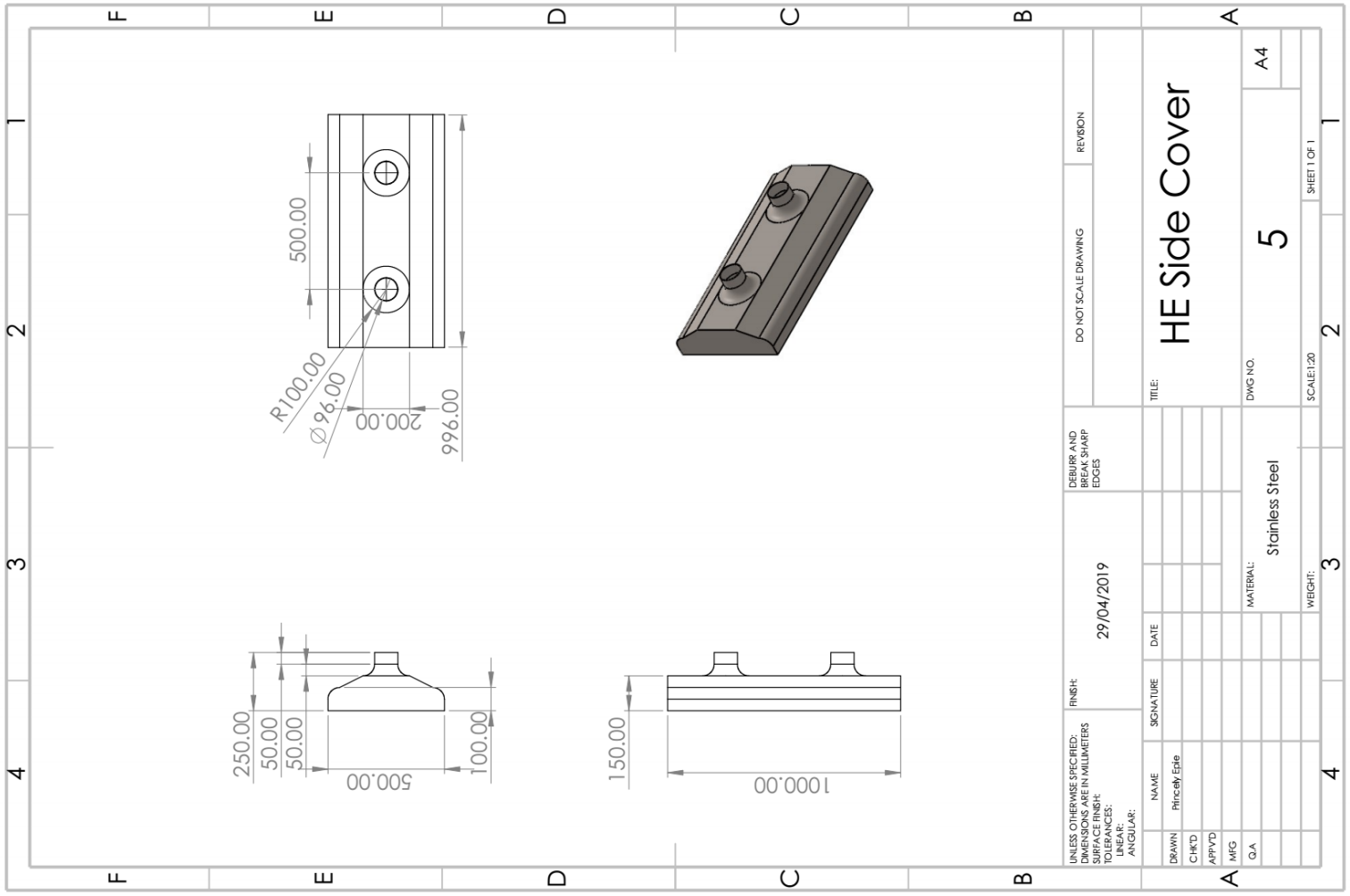

RESUME

I’m Princely Kolle Epie. I was born on the 23.04.1990, Baseng, Cameroon. In the year 2008, I graduated from the Cameroon College of Arts and Science. In 2008 I began my university studies at the University of Buea in the Physics department. In 2009 I moved to the University of Douala where I enrolled into the faculty of Industrial Engineering, department of Automobile Engineering Technology. In 2012 I obtained my Bachelor’s degree from the same department. In the same year (2012), I began a master’s degree in Automobile Engineering Technology and graduated in 2014.

In September 2015 I started working as an Assistant Lecturer at the Catholic University Institute of Buea (CUIB). I worked there for 1 year.

In 2016 I enrolled into Sakarya University for a second master’s degree in Automotive Engineering and started with the Turkish Language Programme. In 2017 I began my university courses in the department of Automotive Engineering.